Supplemental Materials and Methods

Expression and Purification of Recombinant Proteins

We obtained cDNA for *mRFP1* (*mR*) as a kind gift from Prof. R. Y. Tsien (University of California, USA) (47). *8R, TAT, 8K, 8RQ, P21, P21* mutants, *HALO, mNect, Cre, NANOG, MYOD, NEO, mSA2* and *SpAB* cDNAs were synthesized *de novo* (Eurofins MWG Operon). Details of the HBD sequences can be found in Table S1. We cloned cDNAs into the pGEX6-P1 expression vector (Novagen) to create in-frame fusions and expressed proteins in BL21 (DE3) pLysS *Escherichia coli* (Novagen). Exponentially growing LB cultures (OD_{600} = 0.4) shaken at 220rpm at 37˚C were induced using 1 mM IPTG for 24 hours at 25˚C. We lysed and sonicated (7 amplitudes, 1 minute, 5 times) bacterial pellets in 1X STE extraction buffer (50 mM Tris, pH 7.5, 150 mM NaCl, 1 mM EDTA containing 1mM DTT, 0.2 mg/ml lysozyme, and 1X protease inhibitor cocktail). Insoluble protein was retrieved using the Rapid GST inclusion body solubilisation and renaturation kit (AKR-110; Cell Biolabs, Inc., San Diego, CA). We purified recombinant proteins by affinity chromatography using Glutathione-Sepharose resin (GE Healthcare). We removed GST-tags and eluted from resin by PreScission^{TM} Protease cleavage (GE healthcare) in 1X cleavage buffer (50 mM Tris-HCI pH 7.0, 150 mM NaCl, 1 mM EDTA and 1 mM DTT). We determined protein concentration using a BCA-based protein assay (BioRad) with absorbance measured at 595nm using recombinant mR protein as a standard. Integrity and full-length protein expression was confirmed by SDS-PAGE. We determined the fluorescence of recombinant proteins (excitation: 584 nm; emission: 607 nm) with all preparations <10% intensity difference between samples (fluorescence/µg). Standards and samples were analysed using the TECAN

infinite 200PRO multimode reader. Aliquots were stored at -80˚C. P21-8R, LK15 and P21-LK15-8R peptides were synthesised using FMOC chemistry and purified to be >90%.

Cell Culture

Cell lines were obtained from the ATCC. NIH3T3 mouse fibroblast cells (CRL-1658), HEK293T human embryonic kidney cells (CRL-3216), C2C12 mouse myoblast cells (CRL-1772), iHMSC immortalised human mesenchymal stem cells (created as described (48)) and MEF murine embryonic fibroblasts (harvested as described (49)) were maintained in DMEM with 10% (v/v) fetal calf serum (FCS; Sigma) media supplemented with 2mM L-glutamine, 100units/ml penicillin and 100µg/ml streptomycin). CGR-8 mouse embryonic stem cells (mESCs) and *EXT1-/-* mESCs (a kind gift from Dr. D. E. Wells, University of Houston, USA; (21)) were maintained in DMEM, 20% (v/v) FCS, 1000units/ml leukaemia inhibitory factor (LIF), non-essential amino acids, 100µM β-mecaptoethanol (Sigma) 2mM L-glutamine, 100units/ml penicillin and 100µg/ml streptomycin). HL1 mouse cardiomyocyte cells were maintained as described (50). HUES7 human embryonic and IPS2 induced pluripotent stem cells were cultured as previously described (22). HUES7fib human fibroblasts derived from HUES7 cells were generated and cultured as previously described (22). All cells were cultured at 37˚C under 5% CO_2.

Flow Cytometry and Microscopy

For flow cytometry, cells were trypsinized (unless otherwise stated), fixed in 4% (w/v) PFA, resuspended in PBS (pH7.5) and analysed on a MoFlo^{TM} DP (DAKO) Flow Cytometer using a 488nm green laser. (50,000 cells; gated on live cells by forward/side scatter). Median

fluorescence was used for statistical analyses with background from unlabelled/transduced cells subtracted and values taken as ratios to the experimental control. Data shown are three experiments of triplicate samples. For microscopy, cultures were rinsed twice with PBS and imaged with inverted fluorescence microscope (Nikon Eclipse TS100).

Fluorescence Delivery Assay

For testing multiple cell lines we plated 2x 10^5 cells/well (in 12-well plates) onto the surface relevant to the tested cell line, attached cells for 2 hours and transduced with recombinant proteins in cell-type specific growth media. After transduction cells were washed with PBS, trypsinized and fixed in 4% PFA for flow cytometry. For membrane localization, intracellular localisation or both we plated cells as above, but cultures pre-incubated in serum-free media for 1 hour before transduction. Membrane localization to assess cell interaction was achieved by a short transduction of 1 hour in serum-free media. Intracellular localization to assess transduction efficiency was achieved by a short transduction of 1 hour followed by 5 hour incubation in serum-free media only. Cell association (membrane and intracellular levels) were assessed by transducing cells for 6 hours in serum-free medium. For flow cytometry cells were trypsinized, washed and fixed in 4% PFA and for microscopy cells were imaged live after washing in PBS. For trypsin depletion of cell-surface proteins, cells were treated with trypsin/EDTA (Invitrogen) or EDTA-based cell dissociation solution (CDS) (Sigma) for 15 minutes at 37 °C, followed by washes with PBS and 1X soybean trypsin inhibitor (10 mg/ml in PBS; Sigma). Cells were then treated with proteins for 1 hour at 37 °C in serum-free medium. For detergent depletion of cell membranes, cells were treated with PBS (pH7.5) containing 0.1 % (v/v) Triton-X100 (Tx100) for 10 minutes at 37 °C, followed by washes with PBS. Cells were then treated with proteins for 1 hour at 37 °C in serum-free medium. For GAG-treatment cells were pre-treated with GAGs (Sigma) in DMEM without serum

before transduction and were included in the transduction media. This included heparin (Pig intestine) and chondroitin sulfate A (Bovine trachea), B (porcine intestine) and C (shark cartilage) at 0-50 µg/ml.

Total delivered Protein Analyses

We plated 5 x 10^6 NIH3t3 cells (in T25 flasks), pre-incubated cells in serum-free DMEM for 1 hour, and transduced them with mR-8R or P21-mR-8R (0-200µg/ml; 1 ml volume) in serum-free DMEM for 6 hours. NIH3t3 cells transduced with SIN-mR lentiviruses were used as a control for the levels achieved by transgenic systems (22, 51). Cells were harvested by trypsinization, fixed in 4% PFA for flow cytometry or washed several times in cold PBS with soluble protein extracted in cold HKM buffer (20mM HEPES, pH 7.5, 5mM KCl, 0.5 mM $MgCl_2$ and 0.5 mM DTT with 1X complete EDTA-free protease inhibitor cocktail) for fluorometry (52). Extracts were sonicated, centrifuged and NaCl added to yield a final concentration of 100mM prior to analyses. Fluorometry was used to compare soluble extracts with purified mRFP protein diluted in HKM buffer with 100mM NaCl as standards. Flow cytometry was used to assess total delivered protein in intact cells.

Media depletion Assessment

We plated 2 x 10^6 NIH3t3 cells or HUES7 HESCs (in 6-well plates), pre-incubated cells in serum-free DMEM for 1 hour, and transduced with recombinant proteins (20µg/ml; 1 ml volume) in serum-free DMEM for 12 hours. Media was harvested and fluorometry was used to compare the remaining fluorescence in media verses that before cell-incubation.

Fluorescence of media pre-incubation was assigned as 100% fluorescence units and background of serum-free media subtracted.

Heparin-binding assay, Heparinase treatment and depletion of P21-binding molecules from Serum

For heparin binding activity we incubated 1ml of recombinant proteins (20µg/ml) in DMEM with 50µl of PBS-washed Heparin-sepharose beads (Sigma) for 1 hour at 37˚C shaking at 100rpm. Media pre- and post-incubation was compared by fluorometry. For Heparinase treatment, we plated NIH3t3 cells at 2 x 10^5/well (in 12-well plates) and were pre-incubated in serum-free media for 1 hour with Heparinase III (0-1 U/ml) or Heparin (0-50µg/ml). Cells were then washed and transduced with mR or P21-mR-8R (20µg/ml in serum-free media or media with different FCS concentrations) containing Heparinase III or Heparin for 12 hours. FCS was depleted of P21-binding material by affinity chromatography. This was achieved by incubating 50 ml FCS with 2 ml Glutathione-Sepharose resin (GE Healthcare) pre-absorbed with GST-P21 protein expressed in *Escherichia coli*.

Macropinocytosis Assessment

To measure the effects of protein transduction on general macropinocytosis, we incubated cells with 100µg/ml FITC-70kDa neutral dextran (Sigma), along with different recombinant proteins (0-10µg/ml) for 1 hour at 4˚C or 37˚C. Cells were trypsinized and washed in PBS before analyses by flow cytometry.

Cre Recombination Assay

To measure Cre Recombinase activity we created the NIH3t3: LSL-eGFP cell line using the pZ/EG plasmid transfection and G-418 selection (53). To confirm Cre activity efficiently led to recombination and eGFP activation we transduced cells with SIN-Cre lentiviruses (as described in Dixon et al. 2011) and confirmed >95% of cells were eGFP-positive 48 hours post-transduction. We plated 2 $x10^5$ cells/well (in 12-well plates), pre-incubated them in DMEM without serum for 1 hour and treated them with Cre proteins (0-500 µg/ml in DMEM without serum). After the Cre incubation (1min to several hours) cells were trypsinized, replated into complete media and incubated for 2 days. Cells were pre-treated with drugs for the stated time-period in DMEM without serum, were included in Cre-transduction medium and were added after replating. Pre-treatments included: heparin (0-50 µg/ml), chondroitin sulfate A, B and C (0-50 µg/ml), chloroquine (0-100µM), cytochalasin-D (0-10 µM), amiloride (0-5 mM), methyl-β-cyclodextrin (0-5mM), and nystatin (0-50µg/ml). After incubations cell were trypsinized, washed, fixed in 4% PFA and % recombined cells was determined by flow cytometry. For mR-Cre-8R and P21-mR-Cre-8R comparisons concentrations of 100µg/ml and 10µg/ml were used, respectively and data was expressed as % maximum recombination (i.e. the % relative to the maximum recombination achieved at the stared dose of Cre).

NEO Antibiotic-Resistance Assay

To measure NEO activity we assessed survival and proliferation of NIH3t3 and MEF in the presence of G-418 antibiotic selection. Cell number, viability and live/dead ratios were measured. To confirm NEO activity efficiently leads to survival and proliferation under G-418 selection of NIH3t3 and MEF cells we transduced cells with SIN-NEO lentiviruses (as

described in Dixon et al. 2009) and confirmed that NEO transduction prevents cell death and retains viability under stringent G-418 selection. This was used in comparisons with NEO protein transductions. We plated 3 x10^5 MEF cells/well or 1 x 10^5 NIH3t3 cells/well (in 12-well plates) and cultured them in DMEM with 10% FCS containing P21-mR-NEO-8R (0-100µg/ml) for 3 days. Cells were replated at 3 x10^5 cells/well for MEF cells or 1 x10^5 cells/well for NIH3t3 cells. Cells were cultured in DMEM with 10% FCS containing P21-mR-NEO-8R (0-100µg/ml) and G-418 sulfate (0-300µg/ml) for a further 3 days feeding daily to kill non-resistant cells. Cells were counted, assessed for viability using trypan blue exclusion or assayed using the LIVE/DEAD staining (54).

NANOG Self-renewal Assay

To measure NANOG activity we used LIF-withdrawal from CGR-8 mESCs and measured alkaline phosphatase (AP) activity, cell numbers and assessed gene expression changes by quantitative-PCR (QPCR). To confirm NANOG activity efficiently leads to rescue of self-renewal without LIF we transduced cells with SIN-NANOG lentiviruses (as described in Dixon et al. 2009) and confirmed that CGR-8 self-renewal was efficiently rescued and this was used in comparisons with NANOG protein transductions. We plated 2 x10^5 cells/well (in 6-well plates), pre-incubated them in growth media with LIF for one passage/3 days containing P21-mR-NANOG-8R (0-50µg/ml) feeding with fresh media daily. Cells were replated at 2 x10^5 cells/well (in 6-well plates) in growth media without LIF (and with LIF as controls) containing P21-mR-NANOG-8R (0-50µg/ml). Cells were fed daily with this media and every 3 days were counted and passaged replating one-tenth of the cells until 3 passages. After the third passage post-LIF withdrawal cells were stained for AP activity (86R-1kit; based on Naphthol AS-BI and fast red violet LB; Sigma)) or processed for QPCR analyses. Relative expression levels (ΔΔCT) were determined QPCR using TaqMan^{TM} Gene

Expression Master Mix and specific TaqMan™ Gene Expression Assays (Applied Biosystems).

MYOD Myogenesis Assay

To measure MYOD activity we used differentiation of HUES7 HESCs and assessed cell morphology, cell multinucleation, gene expression changes by quantitative-PCR (QPCR) and MYOGENIN protein expression. To confirm MYOD activity efficiently leads to myogenic differentiation of HESCs we transduced cells with SIN-MYOD lentiviruses (as described in Dixon et al. 2009) and confirmed that MYOD directs multinucleated myotube differentiation which was used in comparisons with MYOD protein transductions. We plated 1 $x10^6$ cells/well into 0.1% gelatin-coated plates (in 6-well plates) and cultured them in DMEM with 10% FCS for 1 week with one passage using trypsin. Cells were replated at 1 $x10^6$ cells/well into 0.1% gelatin-coated plates and cultured in DMEM with 10% FCS containing P21-mR-MYOD-8R (0-50µg/ml). Cells were fed daily with this media for 7 days. The culture media was then switched to DMEM with 2% horse serum (HS) and cultures maintained for a further 7 days. Cells were then processed for QPCR or fixed in 4% PFA and immunostained (54). Nuclei were labelled using DAPI as previously described (Dixon et al. 2009). The percentage of MYOGENIN-positive nuclei/total nuclei was quantified, with a minimum of 200 nuclei counted per condition. Relative expression levels (ΔΔCT) were determined QPCR using TaqMan™ Gene Expression Master Mix and specific TaqMan™ Gene Expression Assays (Applied Biosystems).

Antibody, Nucleic acid and Nanoparticle delivery

Biotinylated-Goat anti-Rabbit and FITC-Rabbit anti-mouse antibodies (Sigma), pSIN-GFP (Dixon et al. 2014), modified nucleotide RNA (modRNA) for GFP (Miltenyi Biotech) and FAM-labelled siRNA against GAPDH (Sigma), and nanomag-D (250nm) (MircoMod) were complexed with GET-proteins or –peptides and added to cells. For antibodies complexes were allowed to form in growth media for 20mins before cell addition. For nucleic acids a 2:1 peptide:nucleic acid charge ratio was used for complexation. GET- or LIPO2000 (lipofectamine 2000; Invitrogen) transfection used 10µg or 1 µg nucleic acid per transfection of 100,000 hMSCs in 12 well plates. GET-peptide substituted LIPO2000 following the exact manufacturer's instructions. For MNPs, a final concentration of 25µM peptide was used in an EDAC/NHS reaction using 2mg MNPs according to manufacturer's instructions. Prussian blue was carried out using potassium ferrocyanide (2.5% w/v) in 2.5% w/v HCl.

Supplemental Text

GET requires cell membrane Heparan Sulfate for transduction

To confirm the requirement of cell membrane GAGs we tested the effect of enzymatic depletion of cell membrane heparin sulfate-GAGs and competition with soluble GAGs (SI Appendix, Fig S8 & S9). Heparin prevented the cell-surface binding of GET proteins and strongly inhibited transduction (99.8±2.1%; $p<0.001$). Chondroitin sulfate (CS) A, B or C had little effect on either activity (SI Appendix, Fig S8). We were able to confirm that heparin, CS-B and -C have significant activities in inhibiting PTD-only protein transduction (8.1-, 2.4- and 4.1-fold, respectively; $p<0.05$) as in previous studies (1) but that only heparin significantly affected GET (SI Appendix, Fig S8 & S9).

Next we treated cells with HS-lyase enzyme, heparinase III (SI Appendix, Fig S10). Enzymatic removal of cell-surface heparin sulfate-GAGs potently inhibited GET (at 1U/ml 97.2±3.4%; $p<0.001$). In contrast, neuraminidase treatment depleting sialic acid GAGs did not. We extended our analyses to further define the effect of serum on transduction (SI Appendix, Fig S10b) which has previously been shown to inhibit PTD-mediated delivery (2). Serum inhibited GET but by incubating serum with affinity purified-P21 peptide on sepharose we were able to remove serum's inhibitory effect (10% v/v, ~7.3-fold increase with depletion; $p<0.01$) (SI Appendix, Fig S10c). Inhibition could be reconstituted by addition of soluble heparin (SI Appendix Fig S10d). We therefore concluded that serum is likely to contain GAGs which act as competitive molecules for P21-membrane binding required for efficient GET.

Heparan sulfate-GAGs have a complex sugar structure, consisting of a backbone of repeating disaccharides of glucuronic acid (GlcUA) and N-acetylglucosamine (GlcNAc), polymerized by a heteromeric complex of EXT1/EXT2 enzymes (3). We next used *EXT1-/-* mESCs which

lack endogenously synthesized cell membrane heparin sulfate-GAGs (4). When cultured in conventional mESC media (containing 20% w/v FCS) we saw a significantly lower transduction in *EXT1-/-* mESC (~6.8-fold; $p<0.01$) (SI Appendix Fig S8e,f). This was also apparent when cells were cultured in serum-free conditions likely to be due to interference from soluble GAGs in FCS (~5.6-fold; $p<0.01$). GET was not absent in *EXT1-/-* cells (~9.7-fold over mR control levels) nor was the initial binding of P21-containing proteins. We hypothesize this may be due to incorporation of exogenous serum-GAGs into the deficient *EXT1-/-* cell membrane. As further confirmation we treated cells with sodium chlorate, a potent inhibitor of heparan sulfonation which also potently prevented GET delivery (~7.6-fold; $p<0.05$) (SI Appendix, Fig S11).

Collectively these data comprehensively demonstrate that heparan sulfate-GAG depletion/competition specifically affects the efficacy of protein transduction and therefore endogenous GAGs are important molecules for GET.

GET generates higher intracellular protein levels than Lentiviral transgenesis

If PTD-mediated transduction is to be preferential to gene-therapy approaches it must deliver high-levels of functional protein at low extracellular concentrations and be amenable to control of protein levels over short time-frames. We compared the levels achieved in cells by PTD- or GET-delivery to those achieved by efficient lentiviral transduction (5) (SI Appendix, Fig S20). We extracted soluble protein from transduced cells and measured amounts by fluorometry (SI Appendix, Fig S20a), or used flow cytometry (SI Appendix, Fig S20b). mR-8R levels were several times lower (~3-fold; $p<0.05$) than that achieved by viral transgenesis even at the highest tested doses (200µg/ml; ~6µM). However GET-protein (P21-mR-8R) was delivered at ~16-fold higher levels ($p<0.001$) than seen expressed in transgenic cells.

Importantly, of the amount of P21-mR-8R protein incubated a significant proportion was recovered as soluble intracellular protein (~46±3.5µg/200µg used; ~23±1.7% recovery). It is important to note that under these conditions transduced cells appear red/purple in colour under normal light, demonstrating the efficient enrichment of large quantities of GET protein in cells.

We went on to examine the rate at which these proteins were concentrated in cells by measuring the depletion of fluorescence in media (SI Appendix, Fig S21). 8R-tagged proteins were depleted by ~12% in NIH3t3- and ~3.5% in HUES7-incubations. P21-tagged proteins were significantly depleted in both cell types (~37% and ~25% in NIH3t3 and HUES7 cells, respectively; $p<0.05$) with GET-proteins depleted from media to the highest levels and majority of protein removed (~72 and ~66% in NIH3t3 and HUES7 cells, respectively; $p<0.01$). No cell controls show this was not mediated by protein degradation.

The time required to deplete half of the fluorescence ($T^1/_2$) of P21-mR-8R was only ~9.4 hours, in comparison to mR-8R which required ~62 hours and untagged protein never achieving half-depletion even after 7 days (SI Appendix, Fig S21). These data are corroborative with the cytometric data proving a rapid and efficient enrichment of significant amounts of exogenous GET-protein into cells. In less than a day, the majority of extracellular protein has been effectively internalised using GET delivery.

GET protein enters cells by lipid raft macropinocytosis

Previously it has been shown that PTD-mediated internalization is via macropinocytosis rather than other endocytotic pathways (1). We next determined whether the cellular uptake of GET-proteins occurs through a specific endocytotic pathway employing the Cre assay

system. Removal of cholesterol from the cell plasma membrane disrupts several lipd raft-mediated endocytotic pathways, including caveolae and macropinocytosis (6-8). We treated NIH3t3: LSL-eGFP cells with methyl-β-cyclodextrin and nystatin to deplete or sequester cholesterol, respectively, then transduced GET-tagged Cre. Both methyl-β-cyclodextrin (SI Appendix, Fig S22a) and nystatin (SI Appendix, Fig S22b) disruption of lipid rafts resulted in a dose-dependent inhibition of functional delivery. These data demonstrates that GET-mediated transduction specifically requires lipid raft-mediated endocytosis.

Macropinocytosis is a rapid, lipid raft-dependent and receptor-independent form of endocytosis which requires actin membrane protrusions that envelope into vesicles termed macropinosomes (7-9). To confirm macropinocytosis was indeed the endocytotic mechanism of GET-mediated Cre delivery we pre-treated cells with compounds that disrupt macropinocytosis (Fig. S22a,b). Amiloride is a specific inhibitor of the Na^+/H^+ exchange required for macropinocytosis (10). Cytochalasin D is an inhibitor of F-actin elongation which is required for macropinosome-linked membrane protrusions (11). Amiloride and cytochalasin D did not disrupt cell binding of GET-proteins but resulted in a dose-dependent reduction of functional transduction into cells (SI Appendix, Fig S22c and S22d, respectively). These data confirm that P21 enhances the macropinocytotic pathway used by PTD to internalize cargo molecules.

We investigated the effects of GET-binding on the induction of macropinocytosis. PTD-mediated transduction has previously been shown to promote the uptake of other proteins by an increase in the overall level of macropinocytosis (1). Other studies (1, 12, 13) have demonstrated that neutral dextrans are taken up by amiloride-sensitive macropinocytosis. Cells were incubated with a fluorescent fluid-phase macropinocytotic maker, FITC-labelled 70 kDa neutral dextran, in combination with GET protein, P21-mR-8R (Fig. S23). P21-mR-8R induced a significant dose dependant increase in fluid-phase dextran uptake over steady-

state control levels. P21-mR-8R enhanced FITC-dextran uptake ~2.5-fold (p<0.05) over the stimulation achieved by the same concentration of mR-8R demonstrating that engagement with GAG through P21 and its subsequent effect on PTD-mediated transduction stimulates macropinocytotic uptake.

It was apparent that the majority of PTD-delivered molecules remain trapped in macropinosomes even after further incubation. This indicated that release from these vesicles is inefficient. If fine-tuned and graded amounts of delivery are to be controlled then it would be beneficial if the majority of internalized protein could be considered as functional. We treated cells with chloroquine, an ion-transporting ATPase inhibitor that disrupts endosomes by preventing their acidification (14) (Fig. S22e). Similar doses have been demonstrated to significantly improve the functional delivery of PTD-delivered proteins (1). Sub-cytotoxic doses of chloroquine (100μM) resulted in a marked increase (95.3±4.8-fold; p<0.001) in functional GET protein delivery at a sub-threshold dose (0.1μg/ml) indicating that this is point in the pathway is still a major issue to resolve for GET medicinal application. Nevertheless the GET system was sufficiently efficient that with chloroquine treatment we achieved significant and measureable levels of recombination (4.8±2.9%; p<0.05) with short (1 hour) incubations of >10pg/ml (>0.3pM) (SI Appendix, Fig S22f). Combination of GET efficiency with endosomal-escape technologies may therefore allow precise and temporally controlled amounts of cargo function in cells.

GET-mediated internalisation is efficient after cell membrane association

Even for incubations using low amounts of GET-protein we observed functional quantities of protein activity within cells however to categorically and stringently prove that most GET protein was indeed efficiently internalising we conducted a series of analyses using reporters

that are responsive to their cellular or extracellular localisation. We used HALO ($Halo^{Tag}$) which is a self-labelling protein derived from DhaA (15). HALO rapidly forms a covalent attachment to synthetic chloroalkane-based ligands; with cell permeant and impermeant ligands available. We confirmed intra- versus extracellular labelling of HALO using transgenic over-expression of untagged HALO (for intracellular) and LAMP2b-HALO which is presented on the external cell membrane (for extracellular) and labeling with cell permeant ($HALO^{TAG}$ Oregon Green) or impermeant ($HALO^{TAG}$ $Alexafluor^{488}$) ligands (SI Appendix, Fig S24). We constructed and recombinantly expressed GET-HALO proteins (SI Appendix, Fig S25a) and delivered them to cells testing the internalisation by sensitivity to labelling with the cell impermeant ligand. One hour incubation demonstrated that GET-proteins remained mainly extracellularly localised and attached to the cell membrane (SI Appendix, Fig S25b). However, with further incubation (1h exposure with 5h further incubation; 1h-5h) GET-protein (P21-HALO-8R) is effectively internalised (remaining cell permeant ligand-sensitive but impermeant ligand-insensitive) (SI Appendix, Fig S25c). We repeated these experiments using the mNectarine (mNect) variant of RFP which is pH-sensitive and loses almost all fluorescence in environments <pH6 (16) (SI Appendix, Fig S26). In agreement with HALO transduction, mNect remained mostly membrane localised after 1 h and its fluorescence sensitive to acidic pH media incubation (pH5.5) (SI Appendix, Fig S26d). After further incubation post-delivery (1h-5h) GET-mNect fluorescence was no longer sensitive to extracellular pH (SI Appendix, Fig S26e); however interestingly the absolute fluorescence levels were significantly decreased when compared to GET-mR, presumably due to the internal pH change the protein is experiencing during endosomal acidification (17). These data demonstrates that GET protein membranes association is rapid and transduction is efficient post-cell binding. We hypothesised that membrane clearance of GET-protein could be a rate-limiting step in the delivery process and tested this by undertaking multiple

transductions (1h) of GET-mR varying the time between transductions (SI Appendix, Fig S27a). Indeed re-transduction directly after the initial transduction decreases the effectiveness of the second transduction however as little as 1 h between new transductions is required to obtain a maximal efficiency of re-transduction (SI Appendix, Fig S27b).

GET promotes survival by NEO-conferred resistance of antibiotic selection

The GET system delivers significant amounts of functional protein several orders of magnitude more efficiently than untagged protein and most protein bound to cells is efficiently internalised. Next we sought to determine if prolonged delivery of protein activity could achieved and used delivery of an antibiotic (Neomycin phosphotransferase, NEO) resistance protein to cells under drug selection as an assay (SI Appendix, Fig S28). Significant quantities of NEO protein over several days is required to negate the activity of the antibiotic G-418 sulfate (Geneticin), an aminoglycoside antibiotic, which blocks polypeptide synthesis by inhibiting chain elongation (18).

We subjected both MEF and NIH3t3 cells to transduction with a GET NEO-cargo, P21-mR-NEO-8R followed by simultaneous delivery and G-418 selection (SI Appendix, Fig S20a). We showed a dose-dependent survival of selected cells with transduced P21-mR-NEO-8R (SI Appendix, Fig S28b). This survival was comparable to that conferred transgenically by SIN NEO lentiviral integration (~3.6-fold better survival; $p<0.05$) when P21-mR-NEO-8R was delivered at high doses with lower G-418 doses (~3.3-fold better survival; $p<0.05$) (SI Appendix, Fig S28c-e). The highest-doses of G-418 could only be negated by SIN NEO transgenesis. However, we were able to retain surviving and replicating cells in cultures treated with > LD_{50} G-418 dosages for several weeks. A CPP-version (mR-NEO-8R) of this protein did not confer G-418 resistance (SI Appendix, Fig S16). Taken together, these

experiments provide proof of principle that GET-delivered protein can provide sustained delivery of significant amounts of functional protein assessed using a stringent assay.

Supplemental References

1. Wadia JS, Stan RV, & Dowdy SF (2004) Transducible TAT-HA fusogenic peptide enhances escape of TAT-fusion proteins after lipid raft macropinocytosis. *Nat Med* 10(3):310-315.
2. Kaplan IM, Wadia JS, & Dowdy SF (2005) Cationic TAT peptide transduction domain enters cells by macropinocytosis (vol 102, pg 247, 2005). *J Control Release* 107(3):571-572.
3. Lawrence R, Lu H, Rosenberg RD, Esko JD, & Zhang LJ (2008) Disaccharide structure code for the easy representation of constituent oligosaccharides from glycosaminoglycans. *Nat Methods* 5(4):291-292.
4. Lin X, *et al.* (2000) Disruption of gastrulation and heparan sulfate biosynthesis in EXT1-deficient mice. *Dev Biol* 224(2):299-311.
5. Dick E, Matsa E, Young LE, Darling D, & Denning C (2011) Faster generation of hiPSCs by coupling high-titer lentivirus and column-based positive selection. *Nat Protoc* 6(6):701-714.
6. Anderson RGW (1998) The caveolae membrane system. *Annu Rev Biochem* 67:199-225.
7. Nichols BJ & Lippincott-Schwartz J (2001) Endocytosis without clathrin coats. *Trends Cell Biol* 11(10):406-412.
8. Liu NQ, *et al.* (2002) Human immunodeficiency virus type 1 enters brain microvascular endothelia by macropinocytosis dependent on lipid rafts and the mitogen-activated protein kinase signaling pathway. *J Virol* 76(13):6689-6700.
9. Conner SD & Schmid SL (2003) Regulated portals of entry into the cell. *Nature* 422(6927):37-44.
10. West MA, Bretscher MS, & Watts C (1989) Distinct Endocytotic Pathways in Epidermal Growth Factor-Stimulated Human Carcinoma A431 Cells. *J Cell Biol* 109(6):2731-2739.
11. Sampath P & Pollard TD (1991) Effects of Cytochalasin, Phalloidin, and Ph on the Elongation of Actin-Filaments. *Biochemistry-Us* 30(7):1973-1980.
12. Oliver JM, Berlin RD, & Davis BH (1984) Use of Horseradish-Peroxidase and Fluorescent Dextrans to Study Fluid Pinocytosis in Leukocytes. *Method Enzymol* 108:336-347.
13. Araki N, Johnson MT, & Swanson JA (1996) A role for phosphoinositide 3-kinase in the completion of macropinocytosis and phagocytosis by macrophages. *J Cell Biol* 135(5):1249-1260.
14. Seglen PO, Grinde B, & Solheim AE (1979) Inhibition of the Lysosomal Pathway of Protein-Degradation in Isolated Rat Hepatocytes by Ammonia, Methylamine, Chloroquine and Leupeptin. *Eur J Biochem* 95(2):215-225.
15. Los GV, *et al.* (2008) HaloTag: a novel protein labeling technology for cell imaging and protein analysis. *ACS chemical biology* 3(6):373-382.
16. Johnson DE, *et al.* (2009) Red fluorescent protein pH biosensor to detect concentrative nucleoside transport. *J Biol Chem* 284(31):20499-20511.
17. Gump JM & Dowdy SF (2007) TAT transduction: the molecular mechanism and therapeutic prospects. *Trends in molecular medicine* 13(10):443-448.
18. Eustice DC & Wilhelm JM (1984) Mechanisms of Action of Aminoglycoside Antibiotics in Eukaryotic Protein-Synthesis. *Antimicrob Agents Ch* 26(1):53-60.

Figure S1

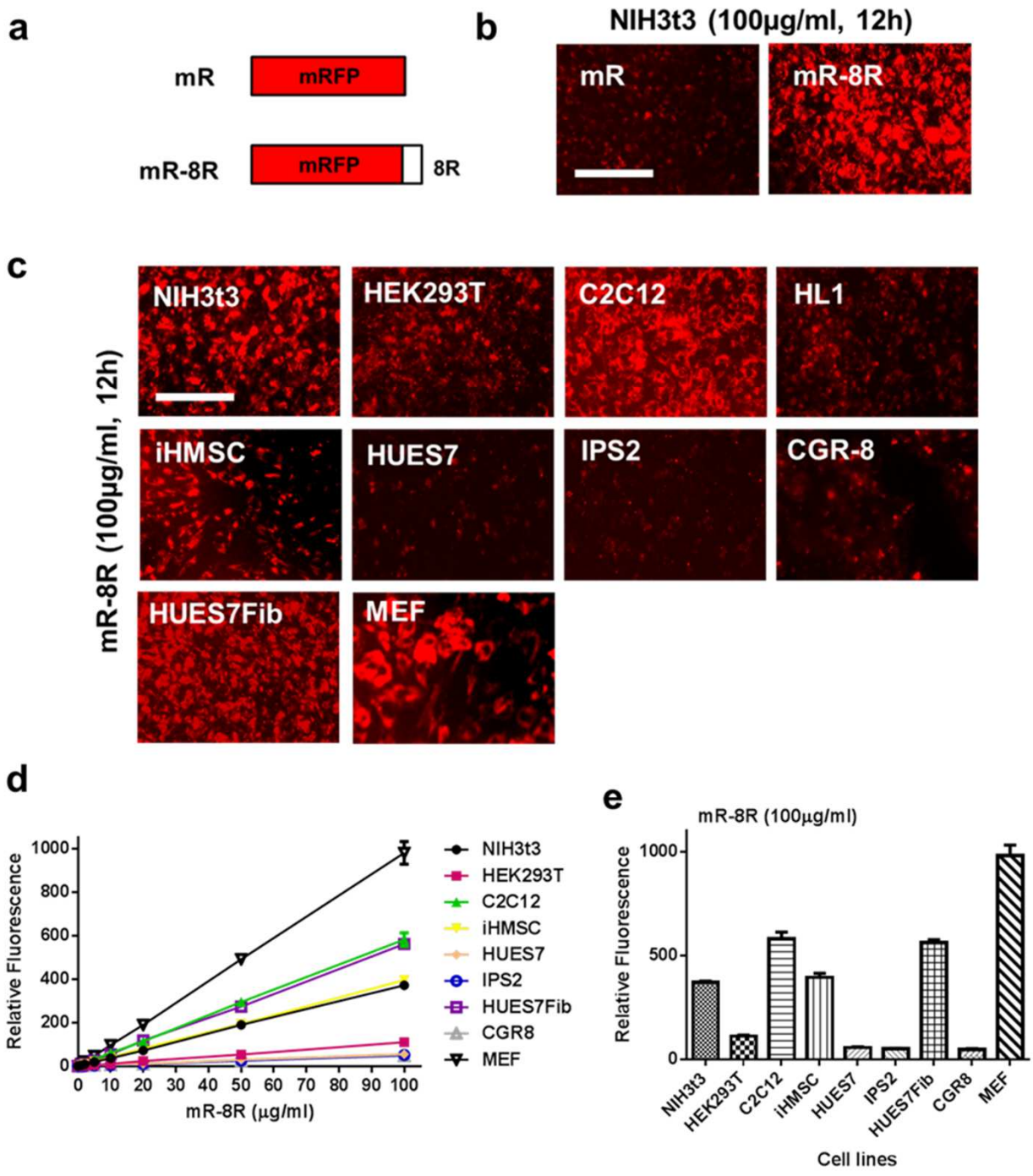
a
mR
mRFP
mR-8R
mRFP
8R
b
NIH3t3 (100μg/ml, 12h)
mR
mR-8R
c
mR-8R (100μg/ml, 12h)
NIH3t3
HEK293T
C2C12
HL1
iHMSC
HUES7
IPS2
CGR-8
HUES7Fib
MEF
d
Relative Fluorescence
1000
800
600
400
200
0
0 10 20 30 40 50 60 70 80 90 100
mR-8R (μg/ml)
NIH3t3
HEK293T
C2C12
iHMSC
HUES7
IPS2
HUES7Fib
CGR8
MEF
e
mR-8R (100μg/ml)
Relative Fluorescence
1000
500
0
NIH3t3
HEK293T
C2C12
iHMSC
HUES7
IPS2
HUES7Fib
CGR8
MEF
Cell lines

Figure S2

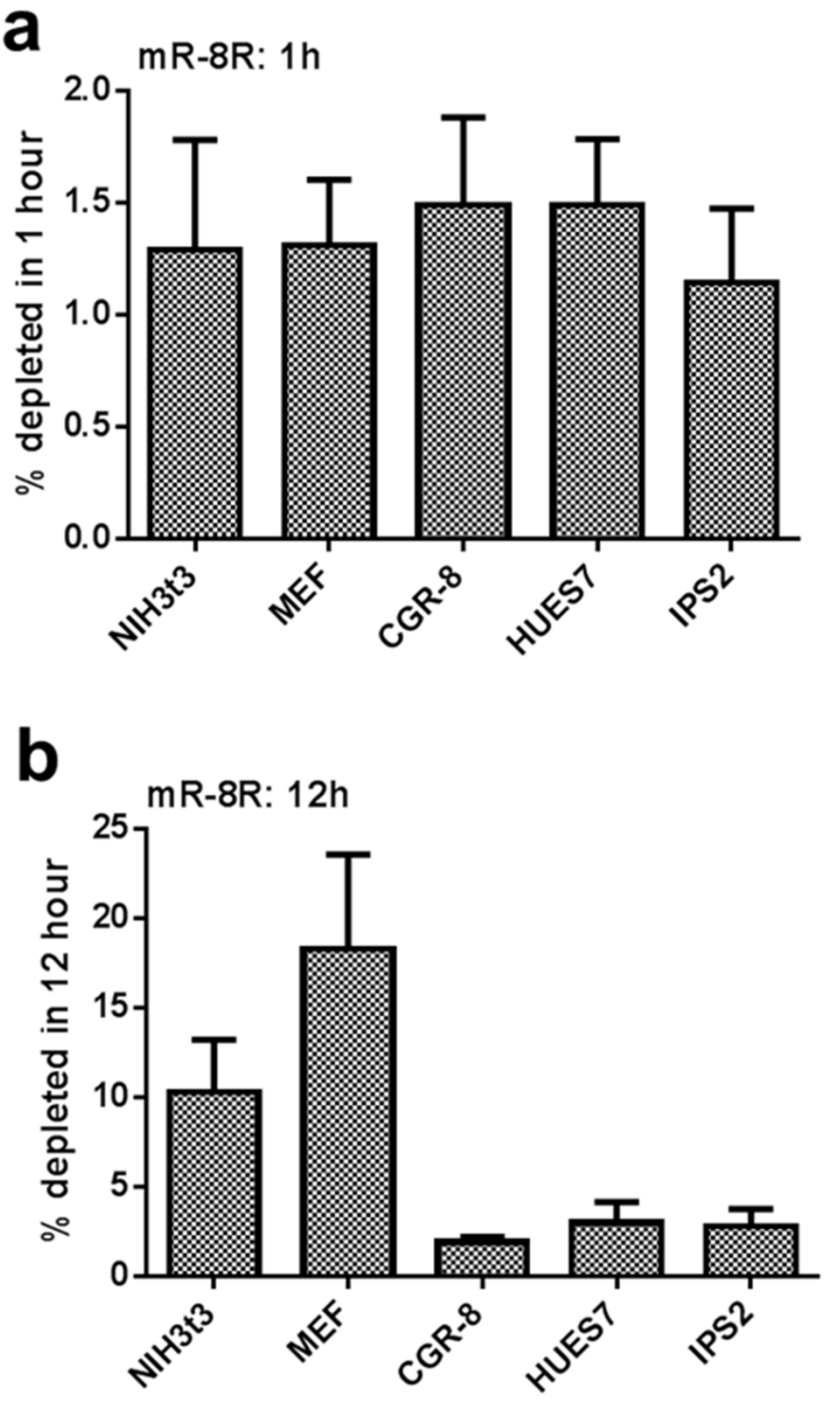
a
mR-8R: 1h
% depleted in 1 hour
2.0
1.5
1.0
0.5
0.0
NIH3t3
MEF
CGR-8
HUES7
IPS2
b
mR-8R: 12h
% depleted in 12 hour
25
20
15
10
5
0
NIH3t3
MEF
CGR-8
HUES7
IPS2

Figure S3

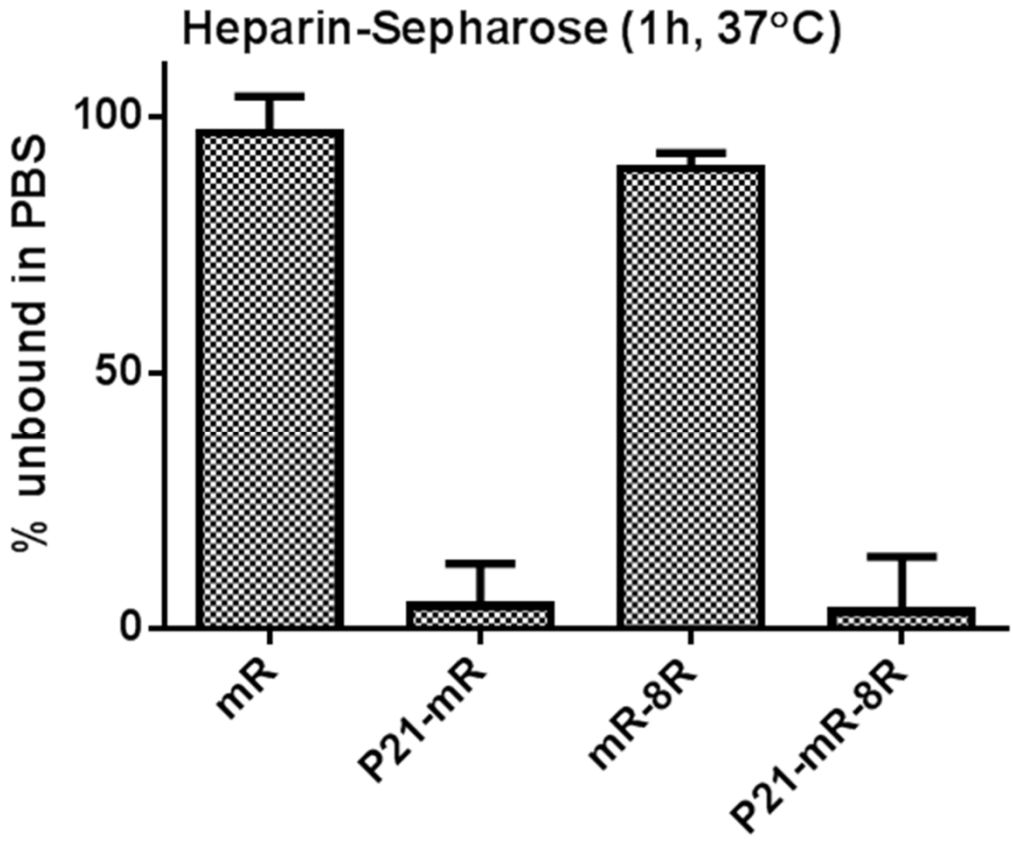
Heparin-Sepharose (1h, 37°C)
% unbound in PBS
100
50
0
mR
P21-mR
mR-8R
P21-mR-8R

Figure S4

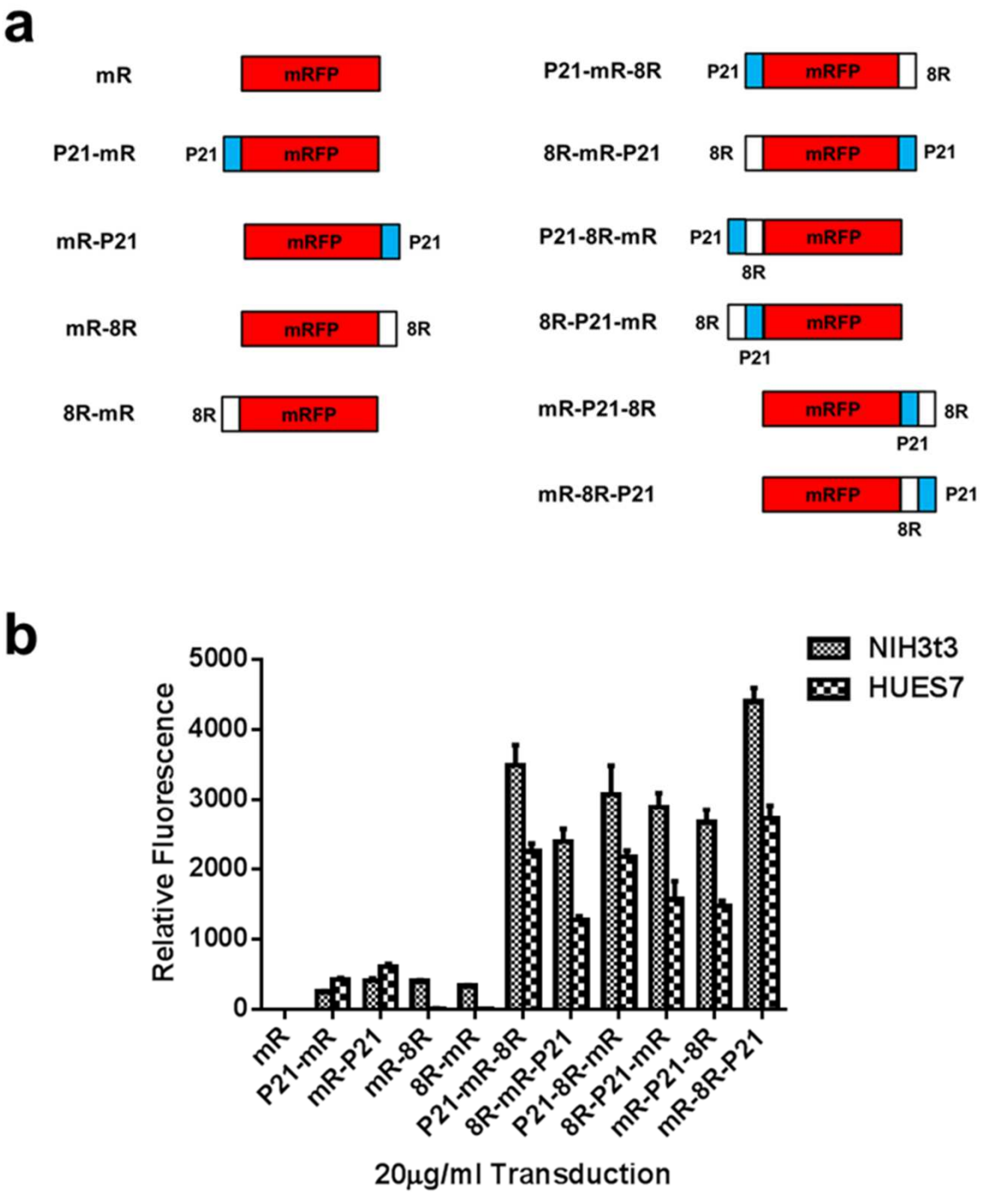
a
mR
mRFP
P21-mR
P21
mRFP
mR-P21
mRFP
P21
mR-8R
mRFP
8R
8R-mR
8R
mRFP
P21-mR-8R
P21
mRFP
8R
8R-mR-P21
8R
mRFP
P21
P21-8R-mR
P21
mRFP
8R
8R-P21-mR
8R
mRFP
P21
mR-P21-8R
mRFP
8R
P21
mR-8R-P21
mRFP
P21
8R
b
NIH3t3
HUES7
Relative Fluorescence
5000
4000
3000
2000
1000
0
mR
P21-mR
mR-P21
mR-8R
8R-mR
P21-mR-8R
8R-mR-P21
P21-8R-mR
8R-P21-mR
mR-P21-8R
mR-8R-P21
20μg/ml Transduction

Figure S5

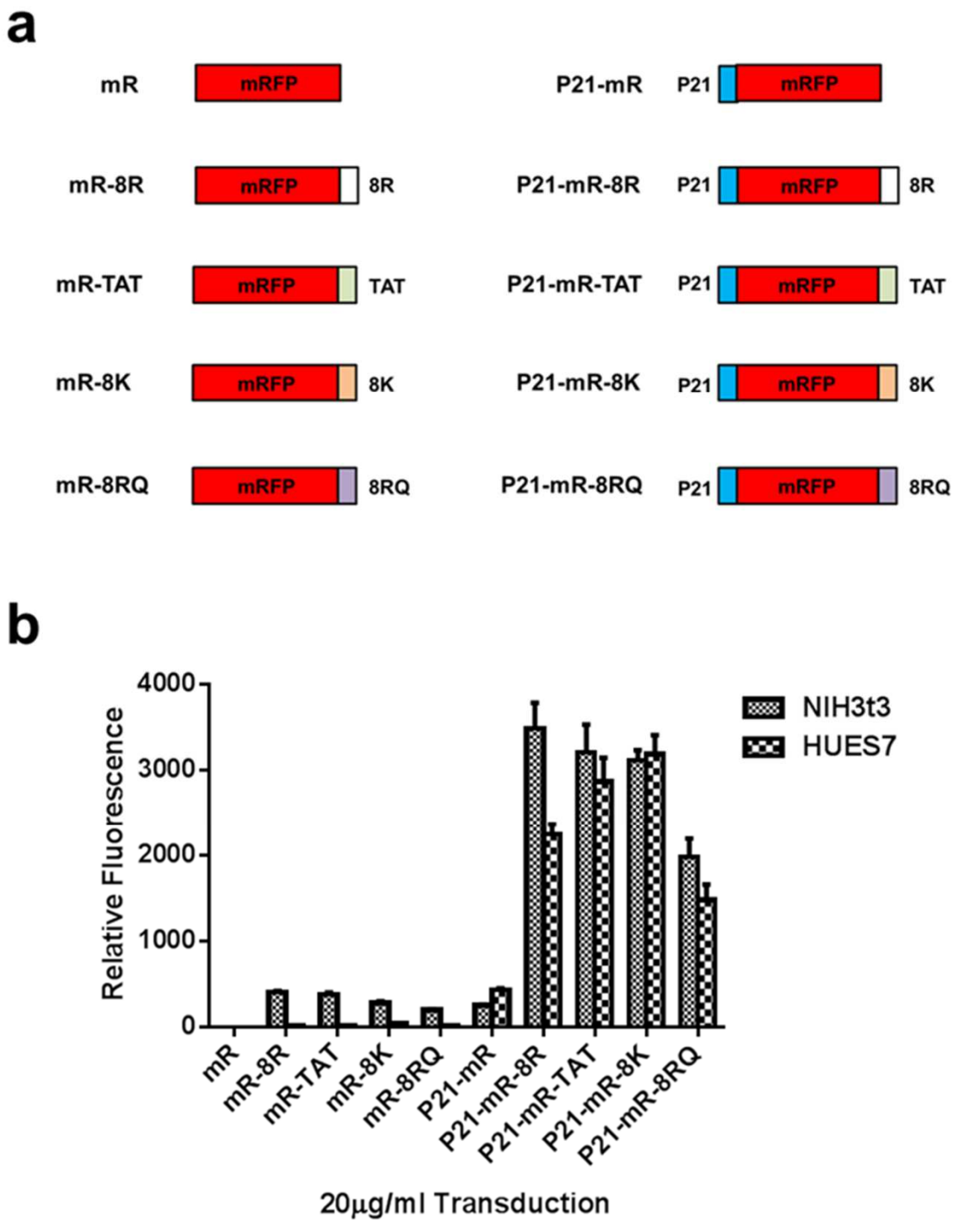
a
mR
mRFP
P21-mR
P21
mRFP
mR-8R
mRFP
8R
P21-mR-8R
P21
mRFP
8R
mR-TAT
mRFP
TAT
P21-mR-TAT
P21
mRFP
TAT
mR-8K
mRFP
8K
P21-mR-8K
P21
mRFP
8K
mR-8RQ
mRFP
8RQ
P21-mR-8RQ
P21
mRFP
8RQ
b
Relative Fluorescence
4000
3000
2000
1000
0
NIH3t3
HUES7
mR
mR-8R
mR-TAT
mR-8K
mR-8RQ
P21-mR
P21-mR-8R
P21-mR-TAT
P21-mR-8K
P21-mR-8RQ
20μg/ml Transduction

Figure S6

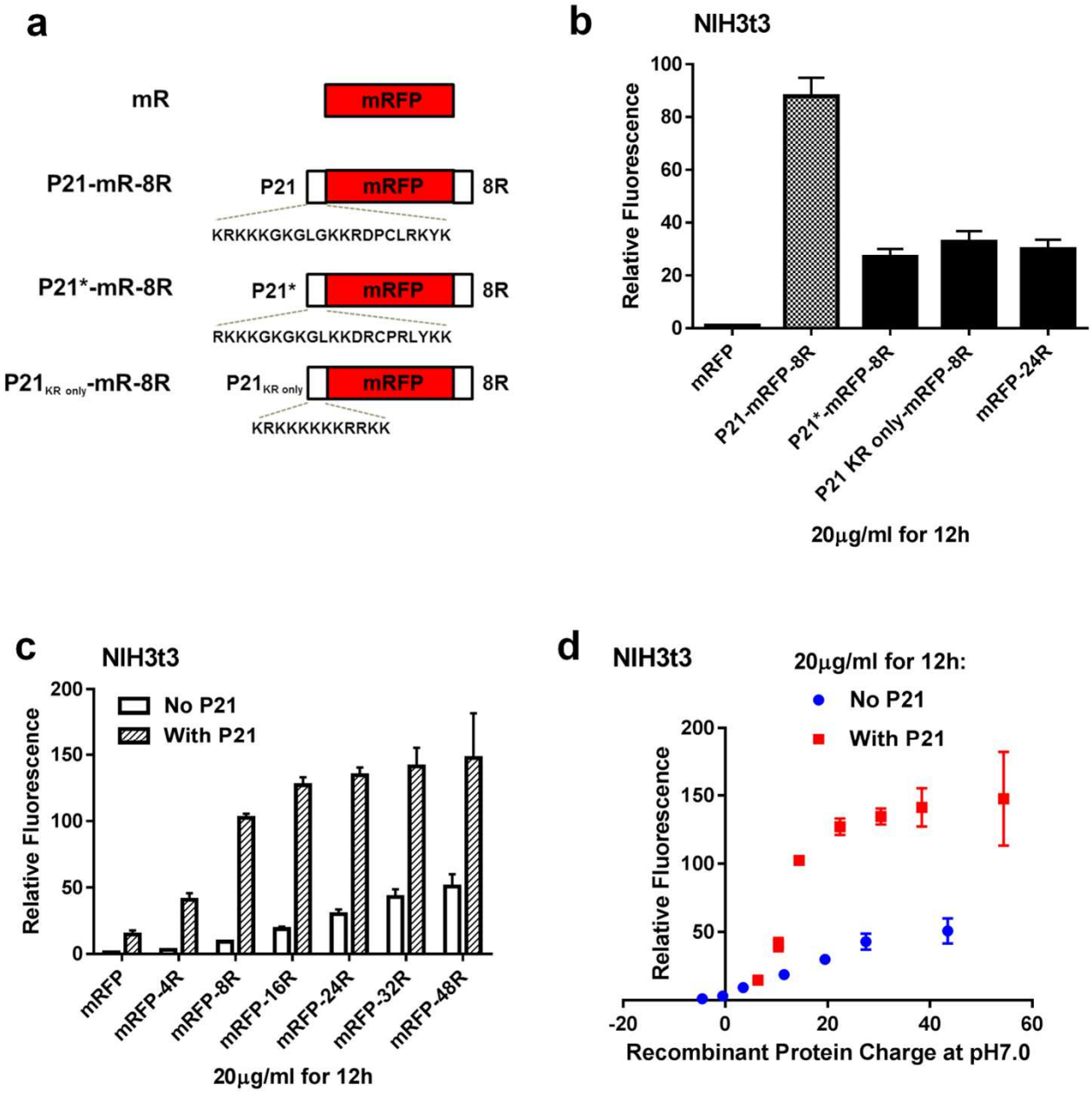
a
mR
mRFP
P21-mR-8R
P21
mRFP
8R
KRKKKGKGLGKKRDPCLRKYK
P21*-mR-8R
P21*
mRFP
8R
RKKKGKGKGLKKDRCPRLYKK
P21KR only-mR-8R
P21KR only
mRFP
8R
KRKKKKKKRRKK
b
NIH3t3
Relative Fluorescence
100
80
60
40
20
0
mRFP
P21-mRFP-8R
P21*-mRFP-8R
P21 KR only-mRFP-8R
mRFP-24R
20μg/ml for 12h
c
NIH3t3
No P21
With P21
Relative Fluorescence
200
150
100
50
0
mRFP
mRFP-4R
mRFP-8R
mRFP-16R
mRFP-24R
mRFP-32R
mRFP-48R
20μg/ml for 12h
d
NIH3t3
20μg/ml for 12h:
No P21
With P21
Relative Fluorescence
200
150
100
50
-20
0
20
40
60
Recombinant Protein Charge at pH7.0

Figure S7

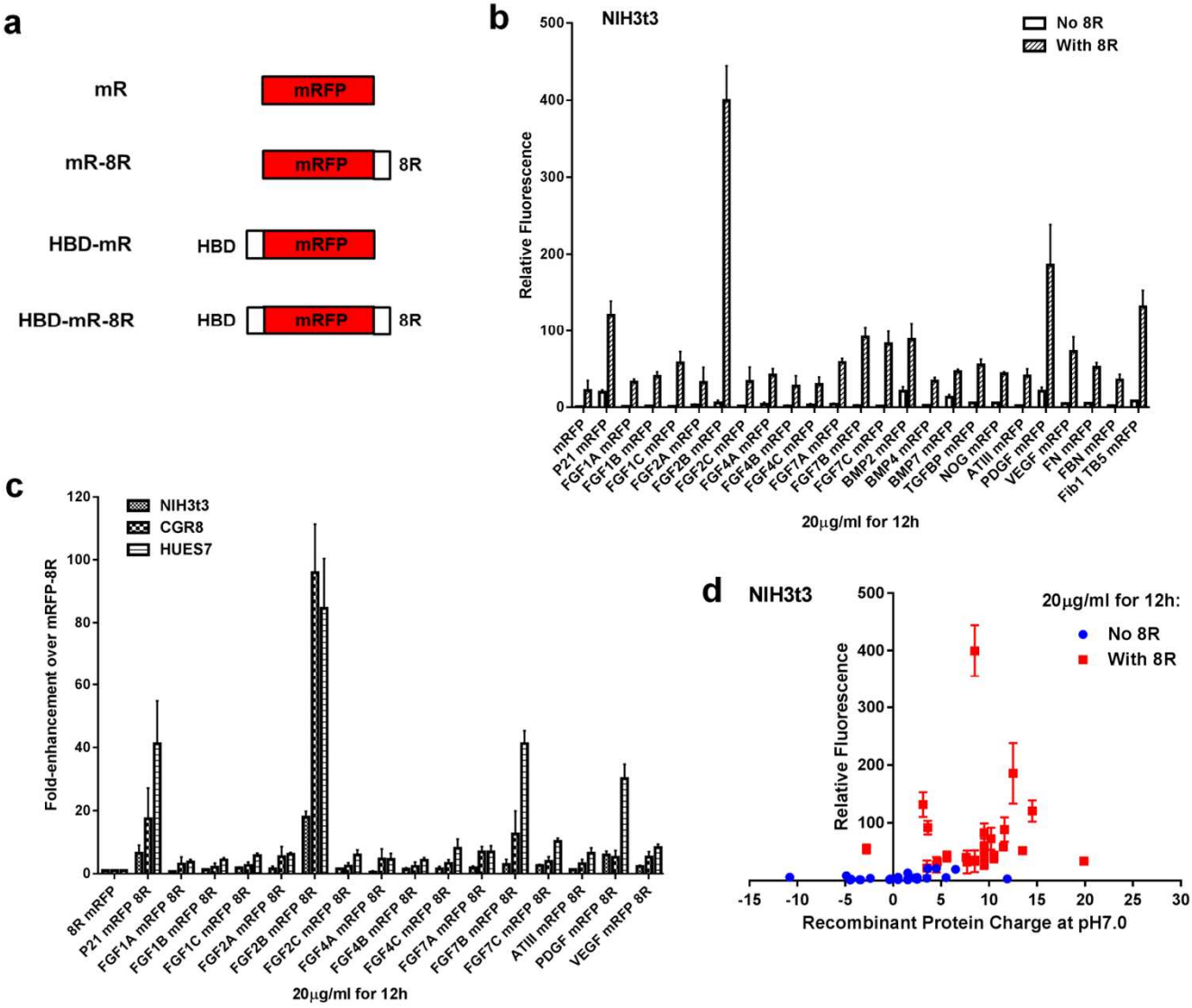
a
mR
mRFP
mR-8R
mRFP
8R
HBD-mR
HBD
mRFP
HBD-mR-8R
HBD
mRFP
8R
b
NIH3t3
No 8R
With 8R
Relative Fluorescence
0
100
200
300
400
500
mRFP
P21 mRFP
FGF1A mRFP
FGF1B mRFP
FGF1C mRFP
FGF2A mRFP
FGF2B mRFP
FGF2C mRFP
FGF4A mRFP
FGF4B mRFP
FGF4C mRFP
FGF7A mRFP
FGF7B mRFP
FGF7C mRFP
BMP2 mRFP
BMP4 mRFP
BMPT mRFP
TGFBP mRFP
NOG mRFP
ATIII mRFP
PDGF mRFP
VEGF mRFP
FN mRFP
FBN mRFP
Fib1 TB5 mRFP
20μg/ml for 12h
c
NIH3t3
CGR8
HUES7
Fold-enhancement over mRFP-8R
0
20
40
60
80
100
120
8R mRFP
P21 mRFP 8R
FGF1A mRFP 8R
FGF1B mRFP 8R
FGF1C mRFP 8R
FGF2A mRFP 8R
FGF2B mRFP 8R
FGF2C mRFP 8R
FGF4A mRFP 8R
FGF4B mRFP 8R
FGF4C mRFP 8R
FGF7A mRFP 8R
FGF7B mRFP 8R
FGF7C mRFP 8R
ATIII mRFP 8R
PDGF mRFP 8R
VEGF mRFP 8R
20μg/ml for 12h
d
NIH3t3
20μg/ml for 12h:
No 8R
With 8R
Relative Fluorescence
0
100
200
300
400
500
-15
-10
-5
0
5
10
15
20
25
30
Recombinant Protein Charge at pH7.0

Figure S8

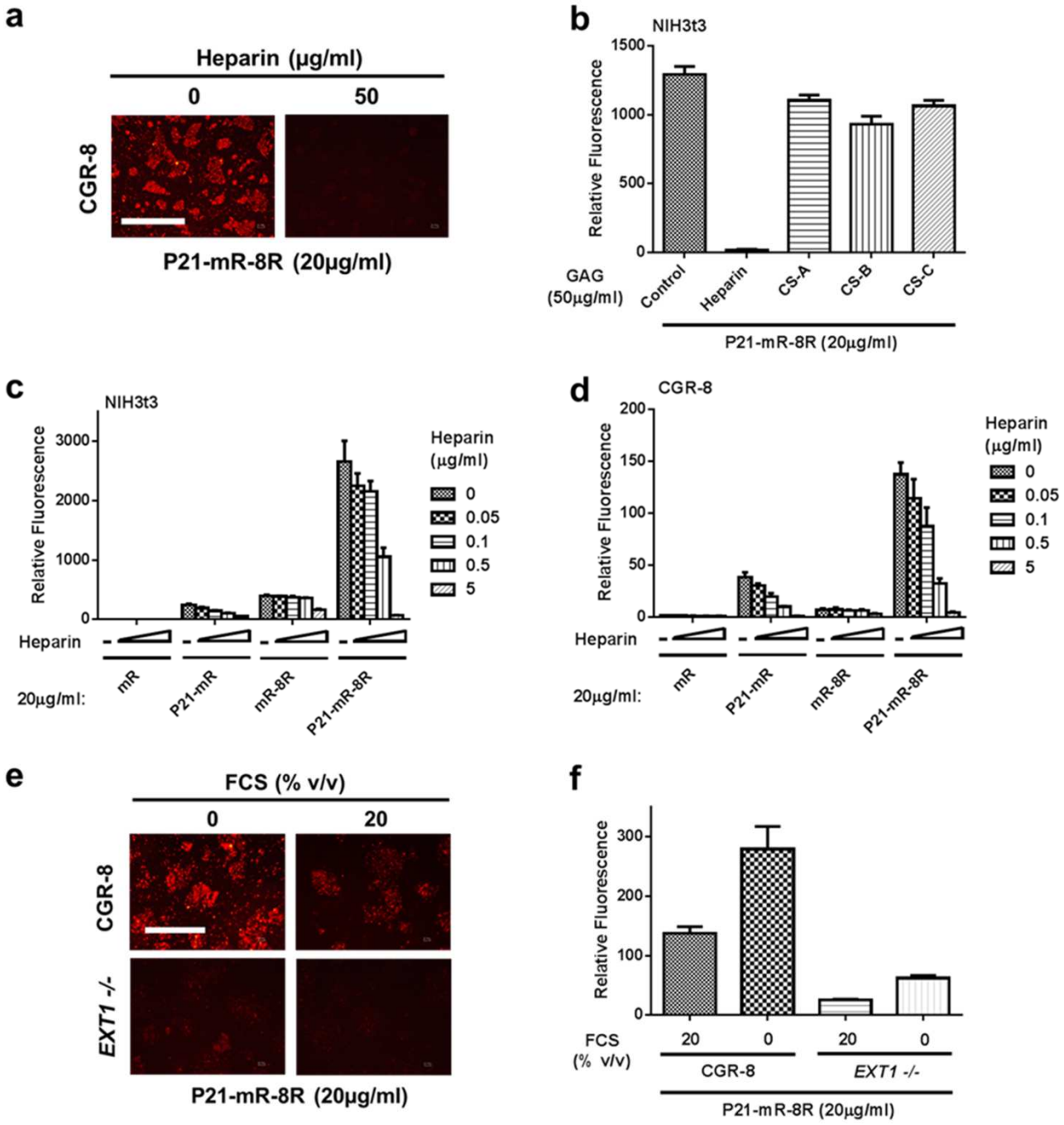
a
Heparin (µg/ml)
0
50
CGR-8
P21-mR-8R (20µg/ml)
b
NIH3t3
Relative Fluorescence
1500
1000
500
0
GAG
(50µg/ml)
Control
Heparin
CS-A
CS-B
CS-C
P21-mR-8R (20µg/ml)
c
NIH3t3
Relative Fluorescence
3000
2000
1000
0
Heparin
(µg/ml)
0
0.05
0.1
0.5
5
Heparin
20µg/ml:
mR
P21-mR
mR-8R
P21-mR-8R
d
CGR-8
Relative Fluorescence
200
150
100
50
0
Heparin
(µg/ml)
0
0.05
0.1
0.5
5
Heparin
20µg/ml:
mR
P21-mR
mR-8R
P21-mR-8R
e
FCS (% v/v)
0
20
CGR-8
EXT1 -/-
P21-mR-8R (20µg/ml)
f
Relative Fluorescence
300
200
100
0
FCS
(% v/v)
20
0
20
0
CGR-8
EXT1 -/-
P21-mR-8R (20µg/ml)

Figure S9

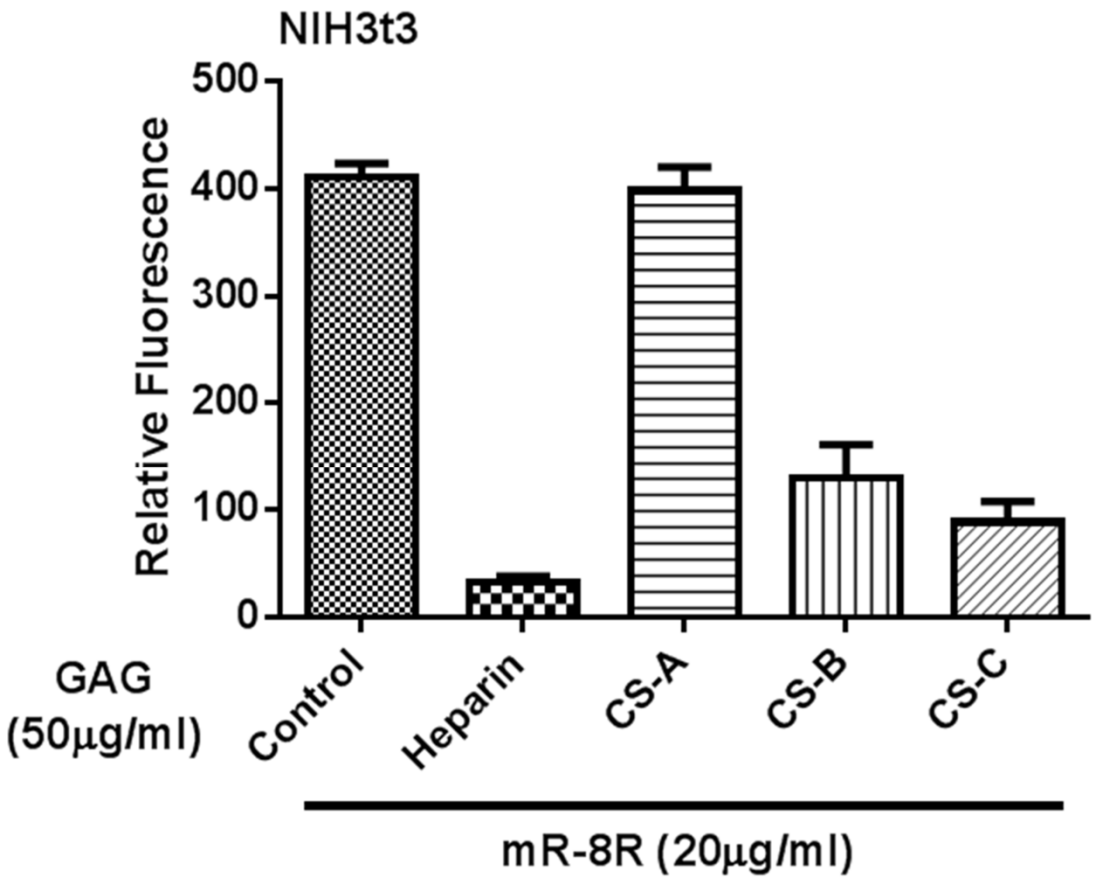
NIH3t3
Relative Fluorescence
500
400
300
200
100
0
GAG
(50μg/ml)
Control
Heparin
CS-A
CS-B
CS-C
mR-8R (20μg/ml)

Figure S10

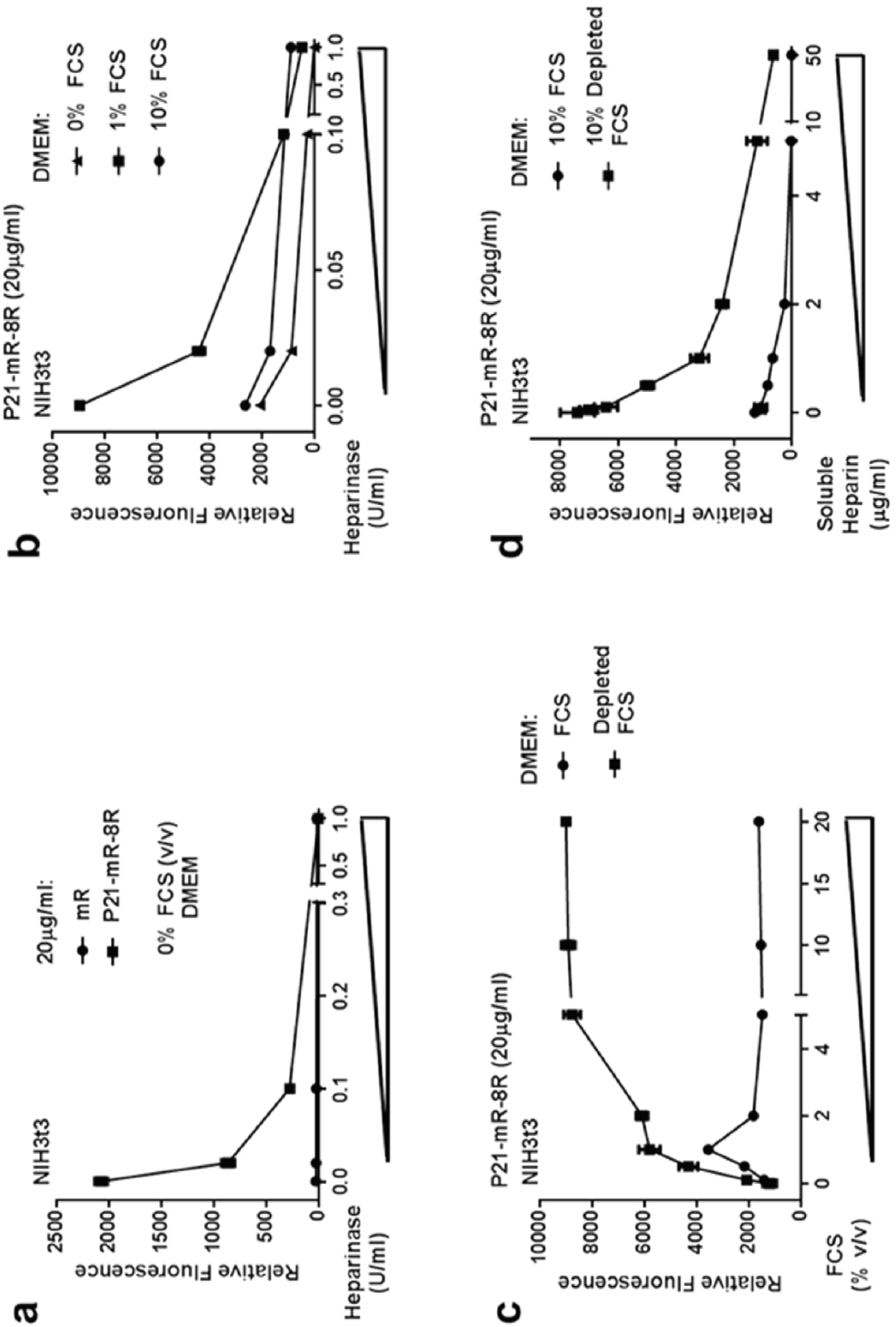
a
NIH3t3
20µg/ml:
mR
P21-mR-8R
0% FCS (v/v)
DMEM
Relative Fluorescence
Heparinase (U/ml)
b
P21-mR-8R (20µg/ml)
NIH3t3
DMEM:
0% FCS
1% FCS
10% FCS
Relative Fluorescence
Heparinase (U/ml)
c
P21-mR-8R (20µg/ml)
NIH3t3
DMEM:
FCS
Depleted FCS
Relative Fluorescence
FCS (% v/v)
d
P21-mR-8R (20µg/ml)
NIH3t3
DMEM:
10% FCS
10% Depleted FCS
Relative Fluorescence
Soluble Heparin (µg/ml)

Figure S11

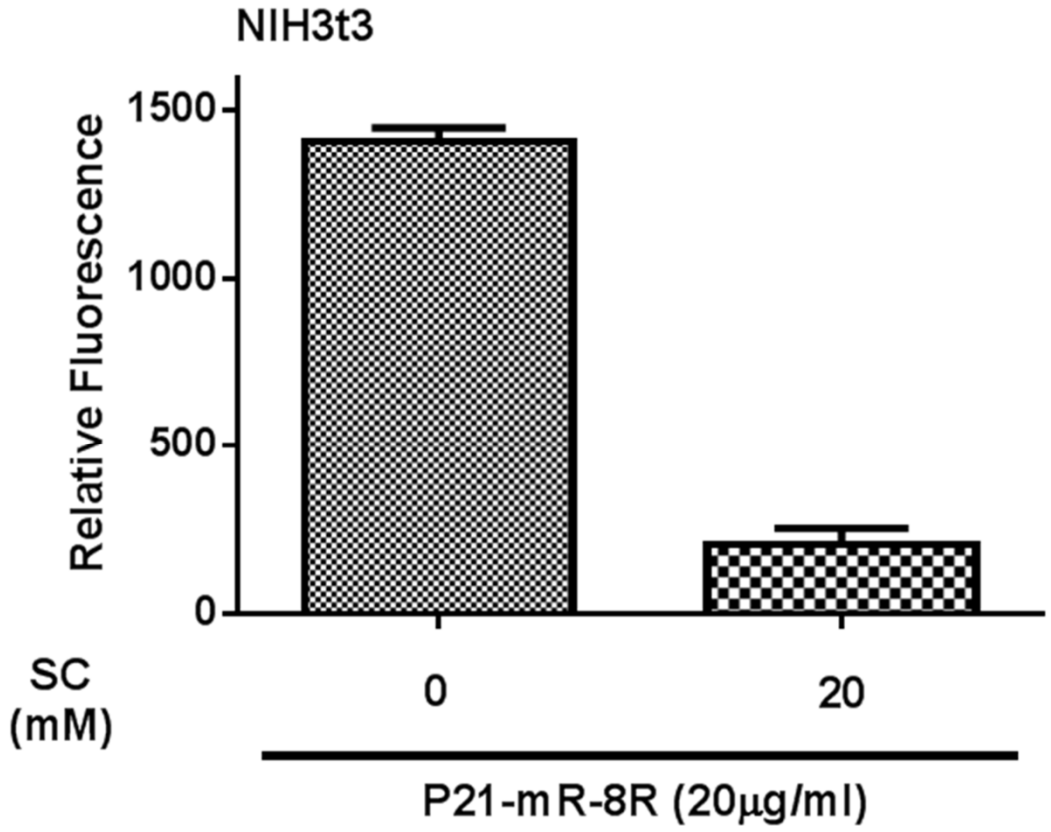
NIH3t3
Relative Fluorescence
1500
1000
500
0
SC
(mM)
0
20
P21-mR-8R (20μg/ml)

Figure S12

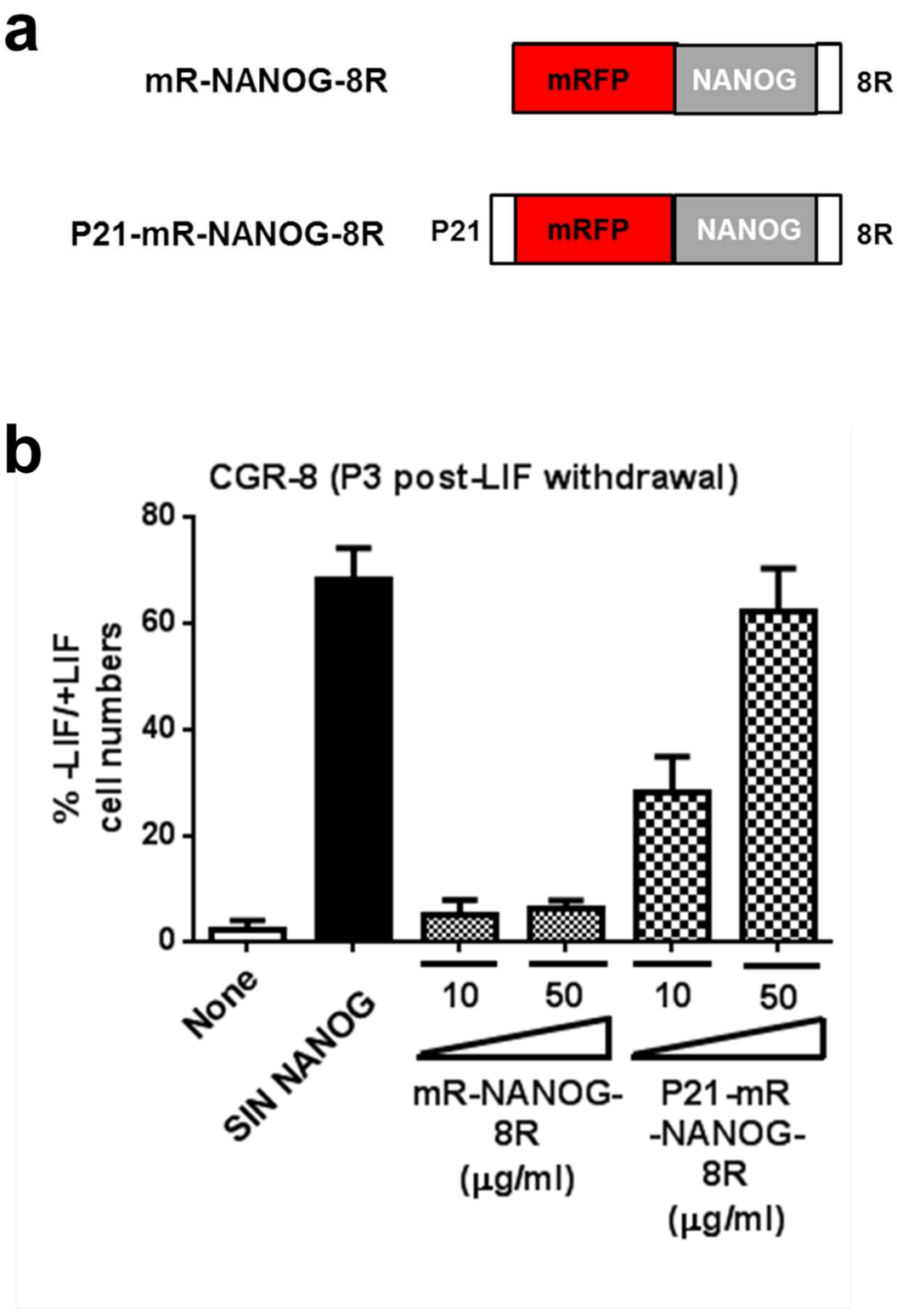
a
mR-NANOG-8R
mRFP
NANOG
8R
P21-mR-NANOG-8R
P21
mRFP
NANOG
8R
b
CGR-8 (P3 post-LIF withdrawal)
% -LIF/+LIF cell numbers
80
60
40
20
0
None
SIN NANOG
10
50
10
50
mR-NANOG-8R (µg/ml)
P21-mR-NANOG-8R (µg/ml)

Figure S13

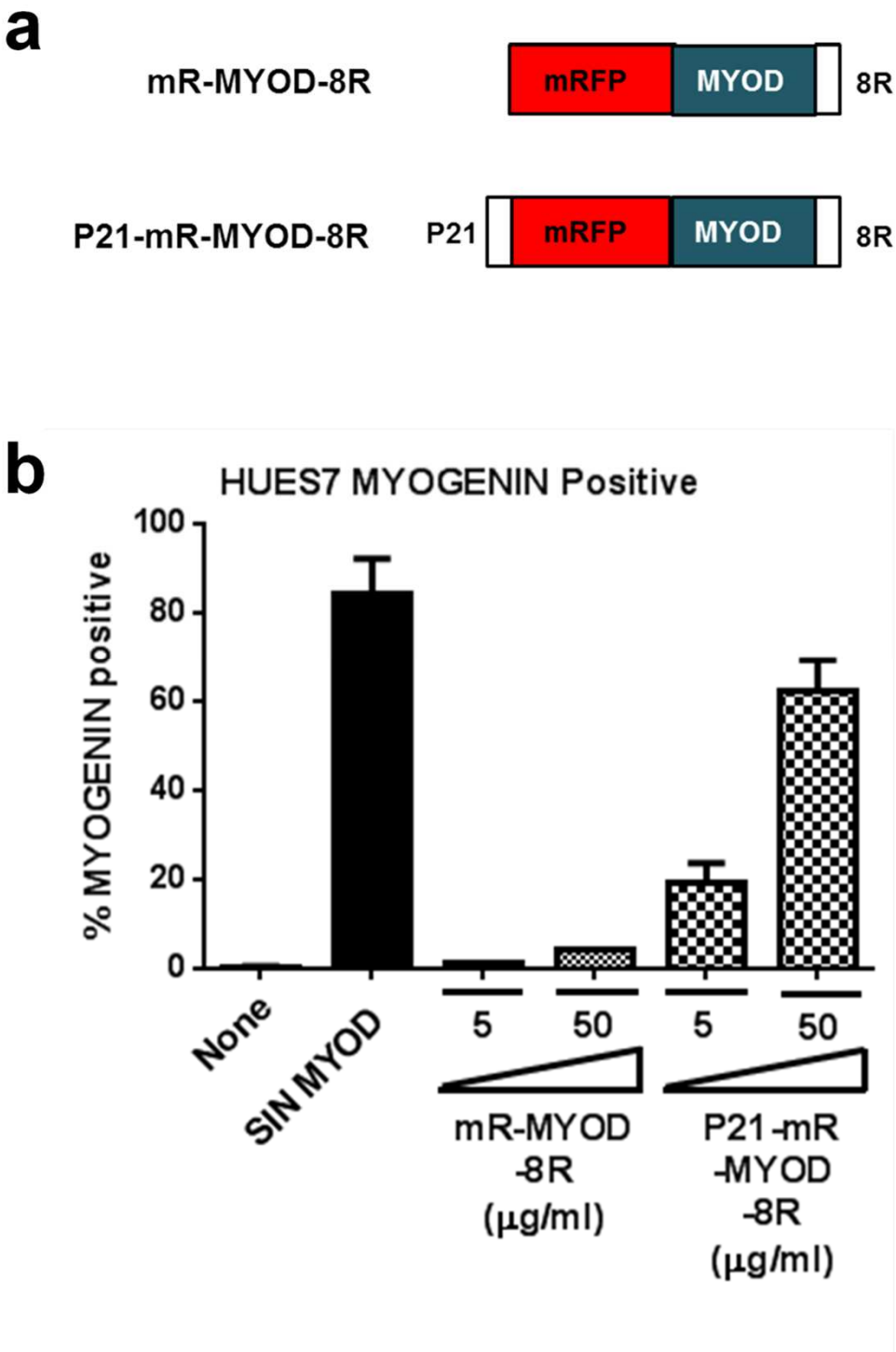
a
mR-MYOD-8R
mRFP
MYOD
8R
P21-mR-MYOD-8R
P21
mRFP
MYOD
8R
b
HUES7 MYOGENIN Positive
% MYOGENIN positive
100
80
60
40
20
0
None
SIN MYOD
5
50
5
50
mR-MYOD -8R (µg/ml)
P21-mR -MYOD -8R (µg/ml)

Figure S14

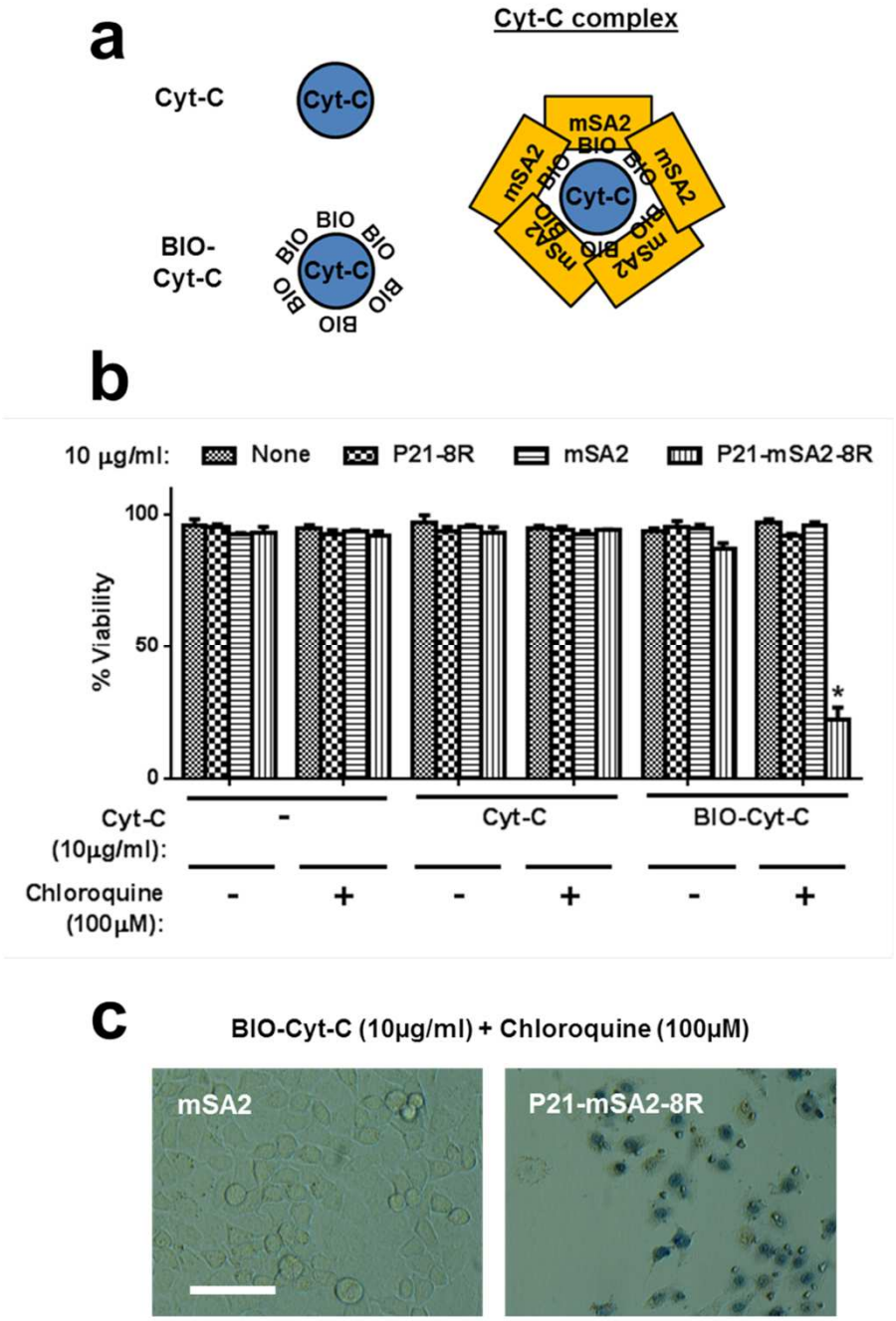
a
Cyt-C complex
Cyt-C
Cyt-C
BIO-
Cyt-C
BIO
Cyt-C
mSA2
BIO
b
10 μg/ml:
None
P21-8R
mSA2
P21-mSA2-8R
100
50
0
% Viability
*
Cyt-C
(10μg/ml):
-
Cyt-C
BIO-Cyt-C
Chloroquine
(100μM):
- + - + - +
c
BIO-Cyt-C (10μg/ml) + Chloroquine (100μM)
mSA2
P21-mSA2-8R

Figure S15

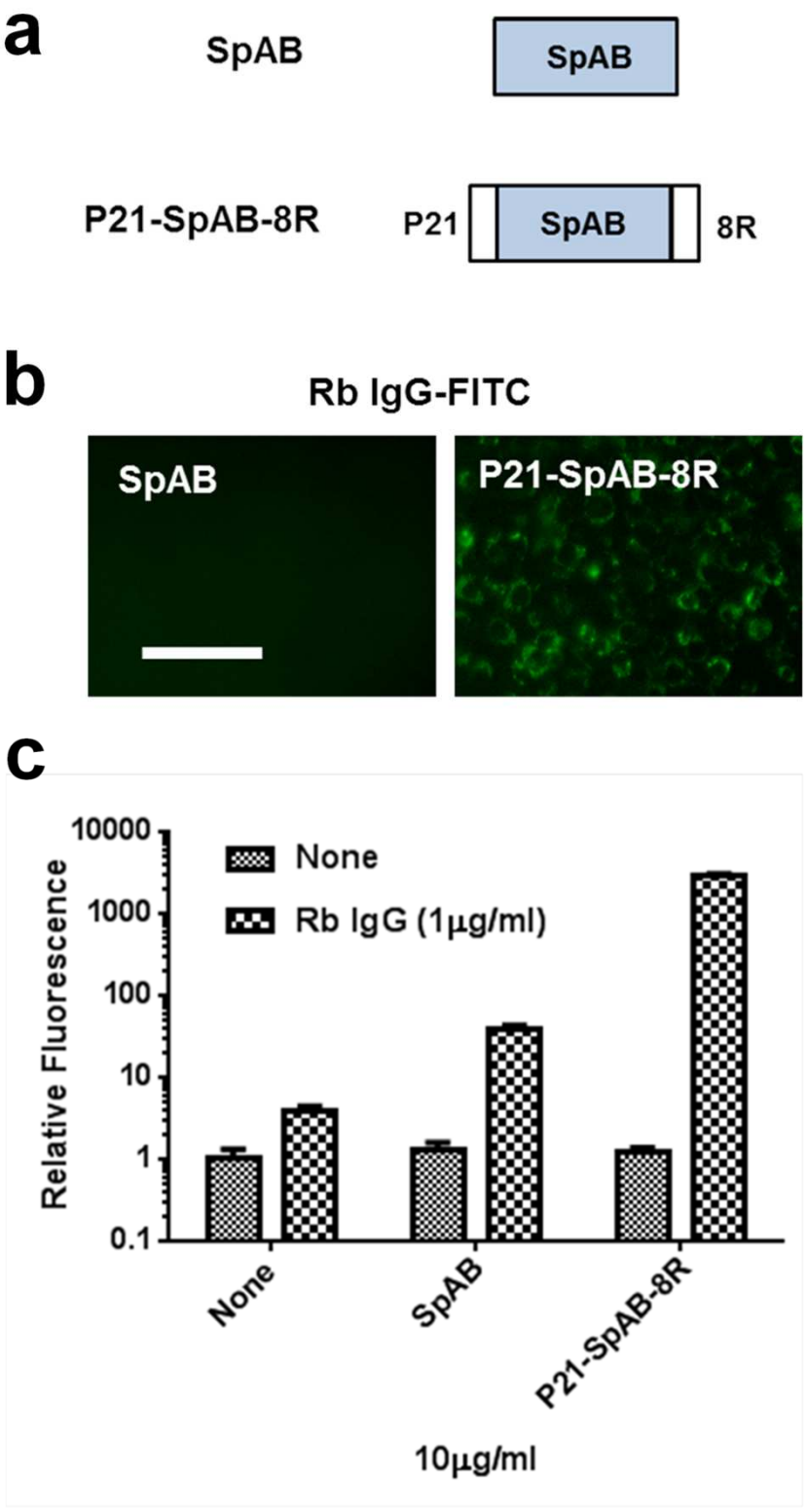
a
SpAB
SpAB
P21-SpAB-8R
P21
SpAB
8R
b
Rb IgG-FITC
SpAB
P21-SpAB-8R
c
Relative Fluorescence
10000
1000
100
10
1
0.1
None
Rb IgG (1μg/ml)
None
SpAB
P21-SpAB-8R
10μg/ml

Figure S16

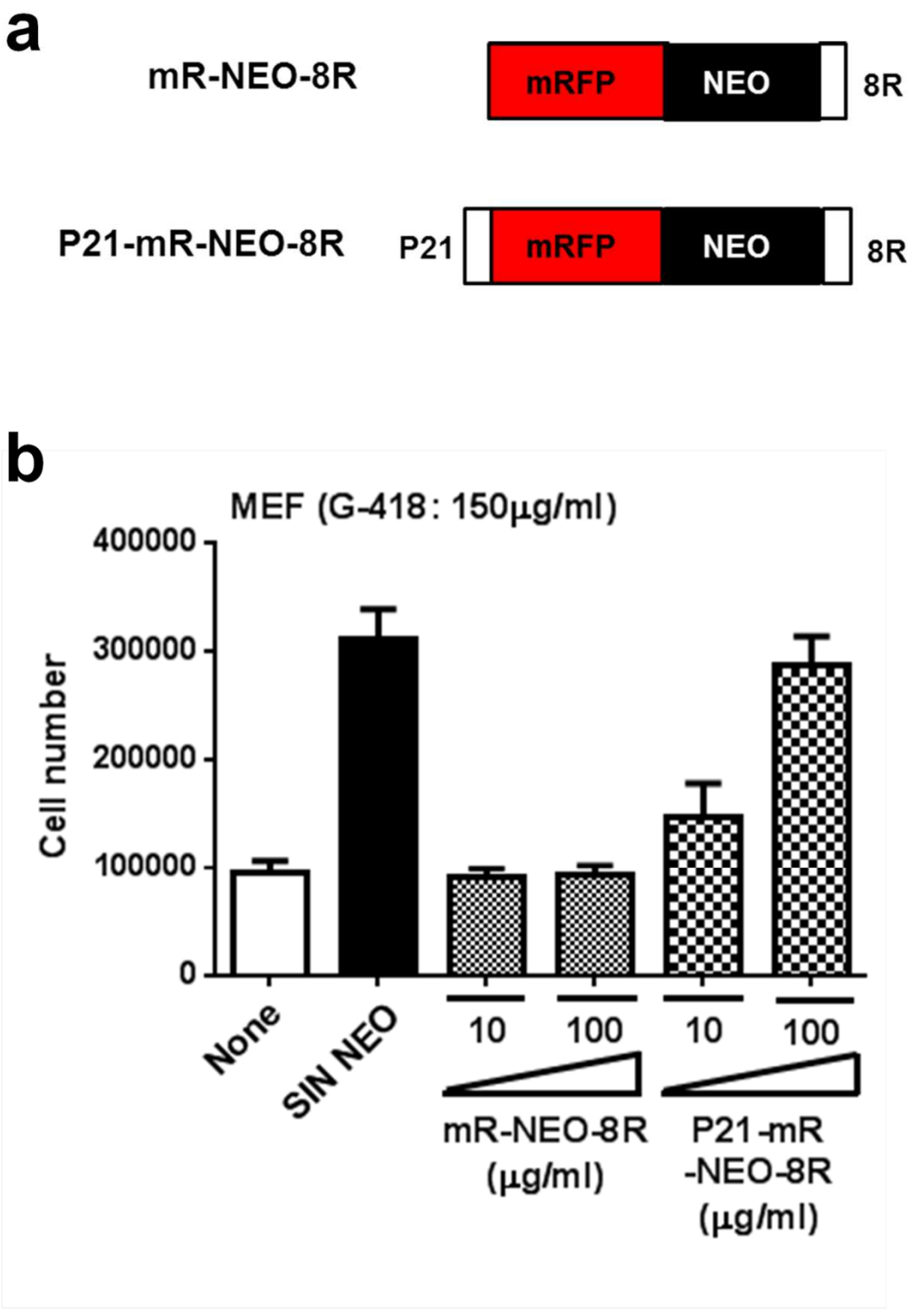
a
mR-NEO-8R
mRFP
NEO
8R
P21-mR-NEO-8R
P21
mRFP
NEO
8R
b
MEF (G-418: 150μg/ml)
Cell number
400000
300000
200000
100000
0
None
SIN NEO
10
100
10
100
mR-NEO-8R (μg/ml)
P21-mR-NEO-8R (μg/ml)

Figure S17

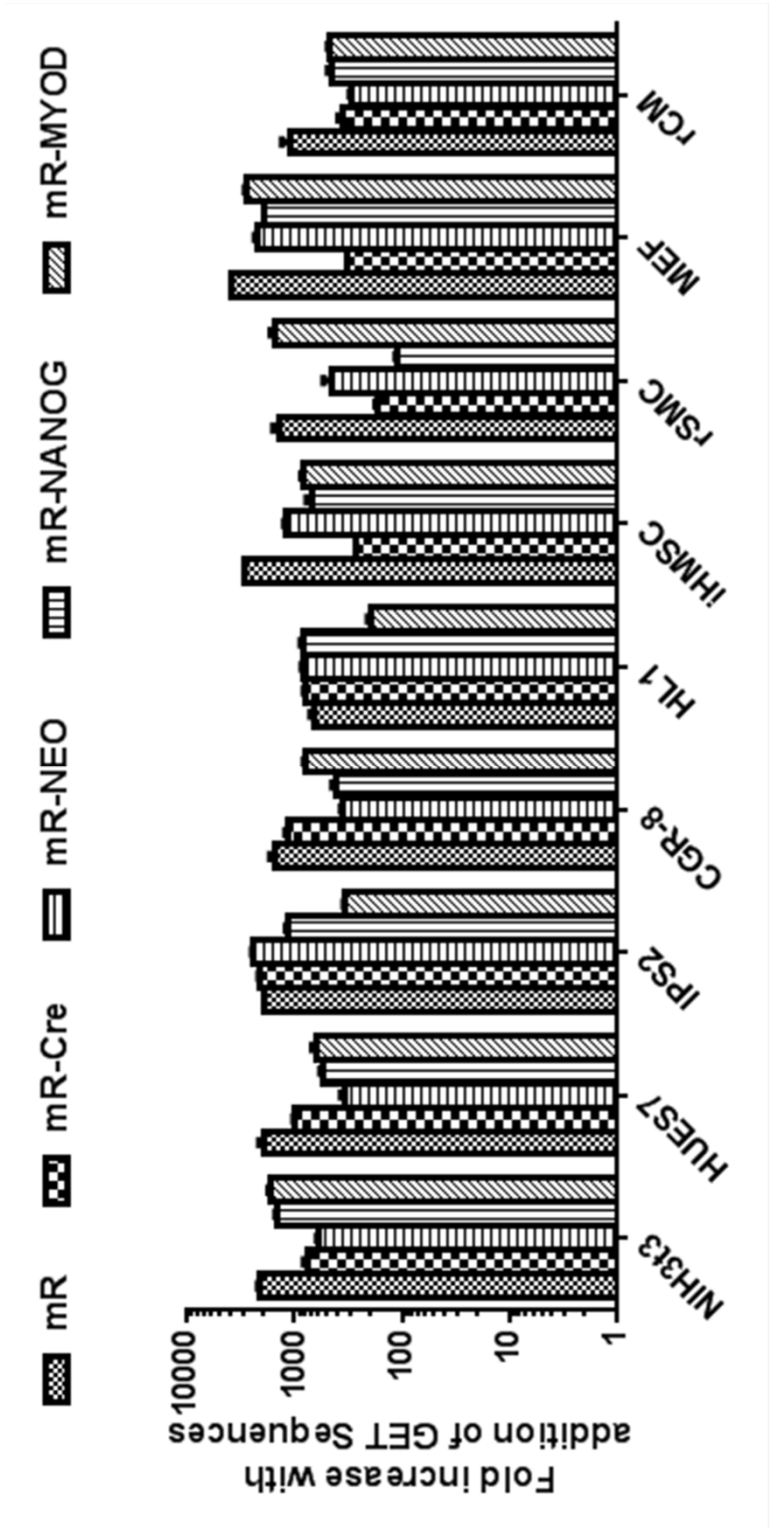
mR
mR-Cre
mR-NEO
mR-NANOG
mR-MYOD
Fold increase with addition of GET Sequences
10000
1000
100
10
1
NIH3t3
HUES7
IPS2
CGR-8
HL-1
iHMSC
FSMC
MEF
rCM

Figure S18

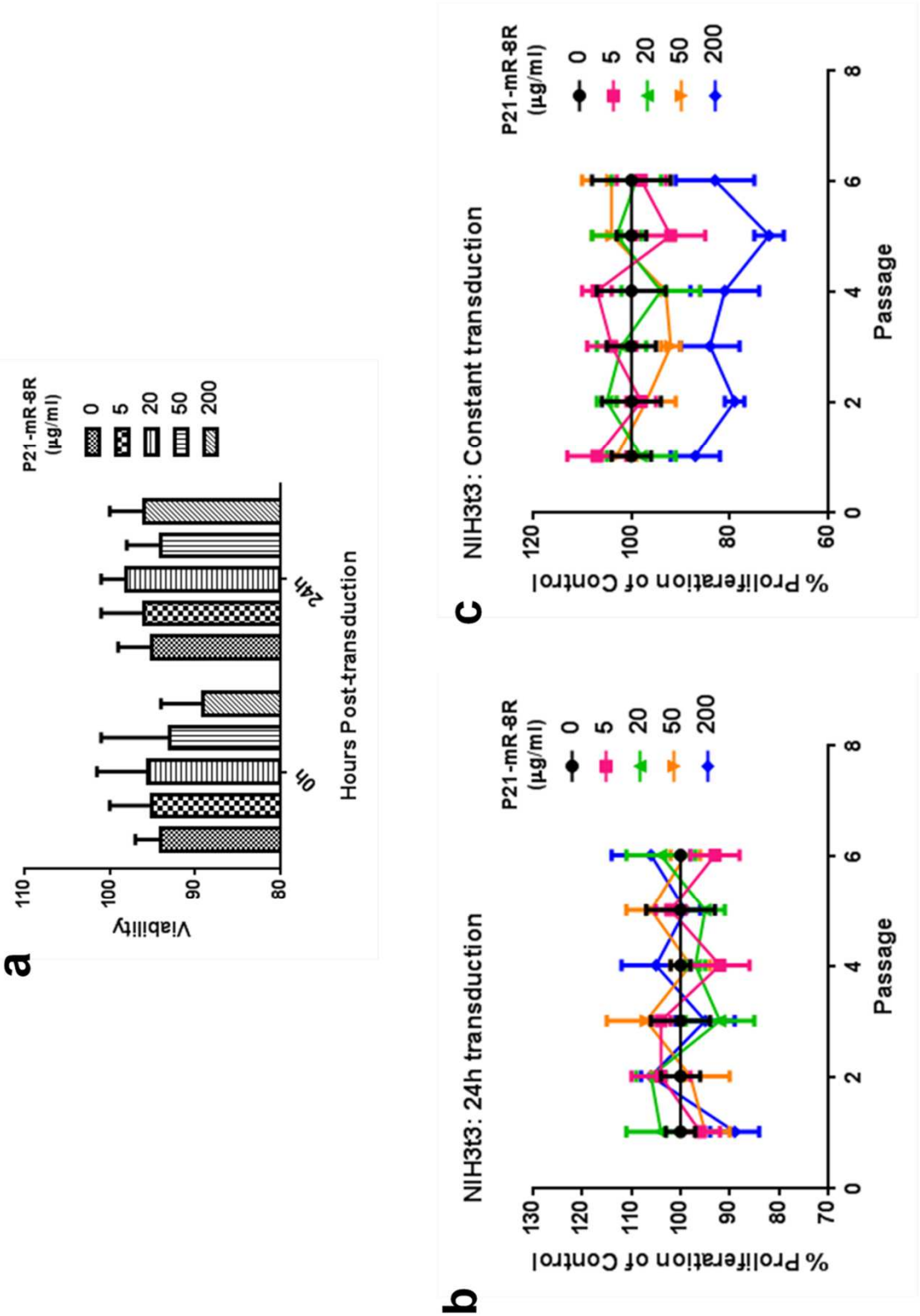
a
Viability
110
100
90
80
0h
24h
Hours Post-transduction
P21-mR-8R (µg/ml)
0
5
20
50
200
b
NIH3t3: 24h transduction
% Proliferation of Control
130
120
110
100
90
80
70
0
2
4
6
8
Passage
P21-mR-8R (µg/ml)
0
5
20
50
200
c
NIH3t3: Constant transduction
% Proliferation of Control
120
100
80
60
0
2
4
6
8
Passage
P21-mR-8R (µg/ml)
0
5
20
50
200

Figure S19

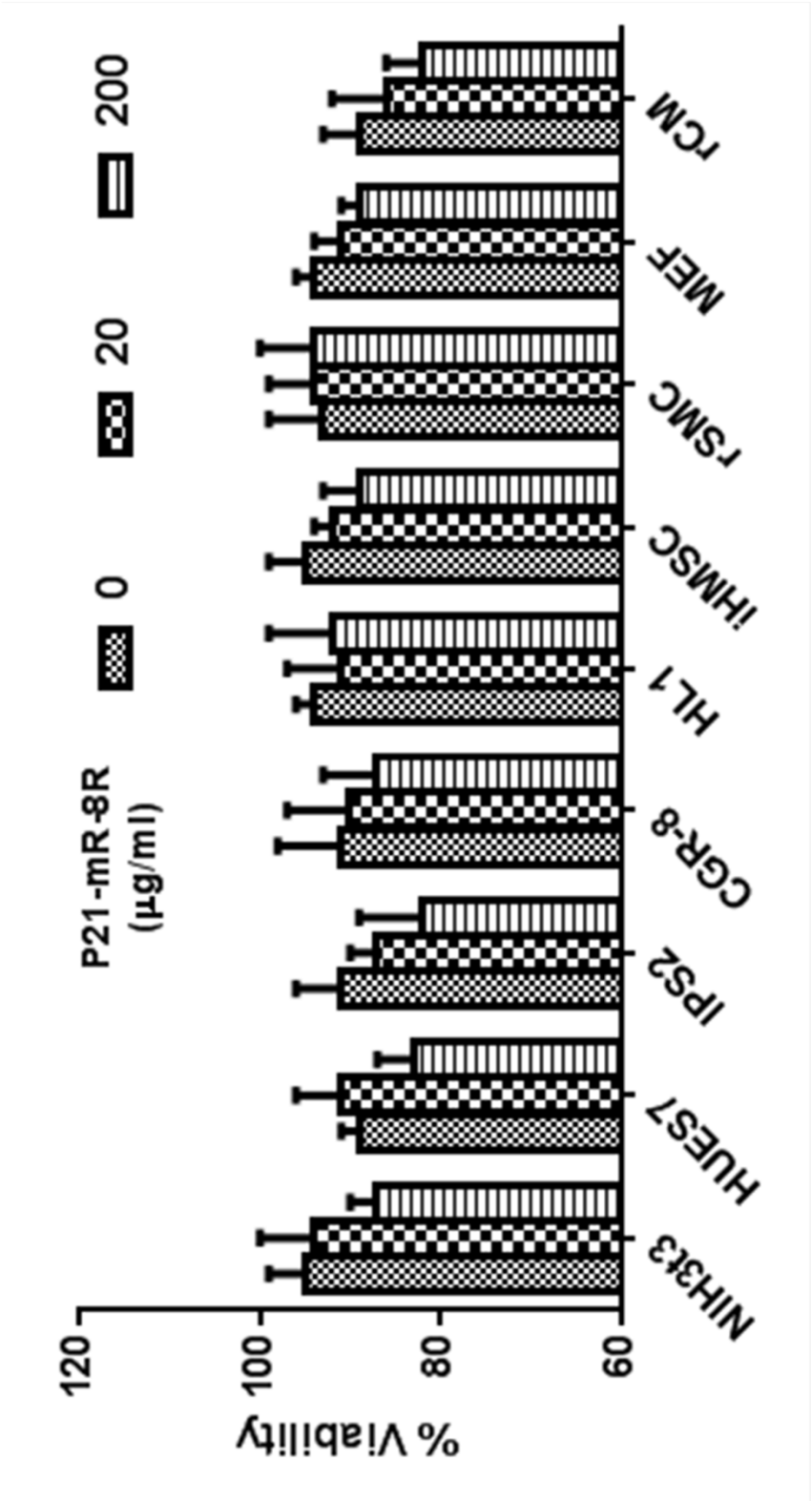
% Viability
120
100
80
60
NIH3t3
HUES7
IPS2
CGR-8
HL-1
iHMSC
rSMC
MEF
rCM
P21-mR-8R (µg/ml)
0
20
200

Figure S20

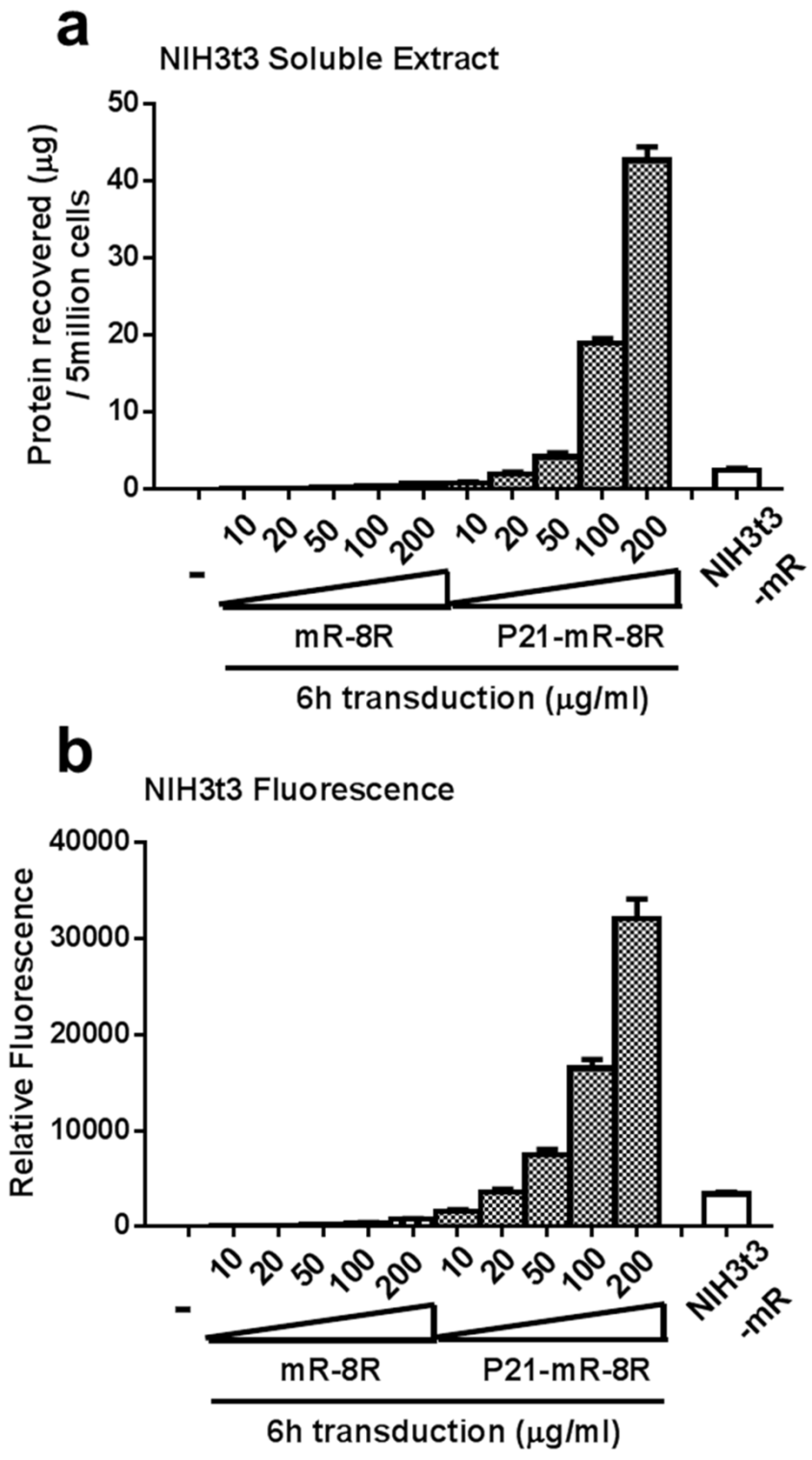
a
NIH3t3 Soluble Extract
Protein recovered (μg)
/ 5million cells
50
40
30
20
10
0
-
10
20
50
100
200
10
20
50
100
200
NIH3t3
-mR
mR-8R
P21-mR-8R
6h transduction (μg/ml)
b
NIH3t3 Fluorescence
Relative Fluorescence
40000
30000
20000
10000
0
-
10
20
50
100
200
10
20
50
100
200
NIH3t3
-mR
mR-8R
P21-mR-8R
6h transduction (μg/ml)

Figure S21

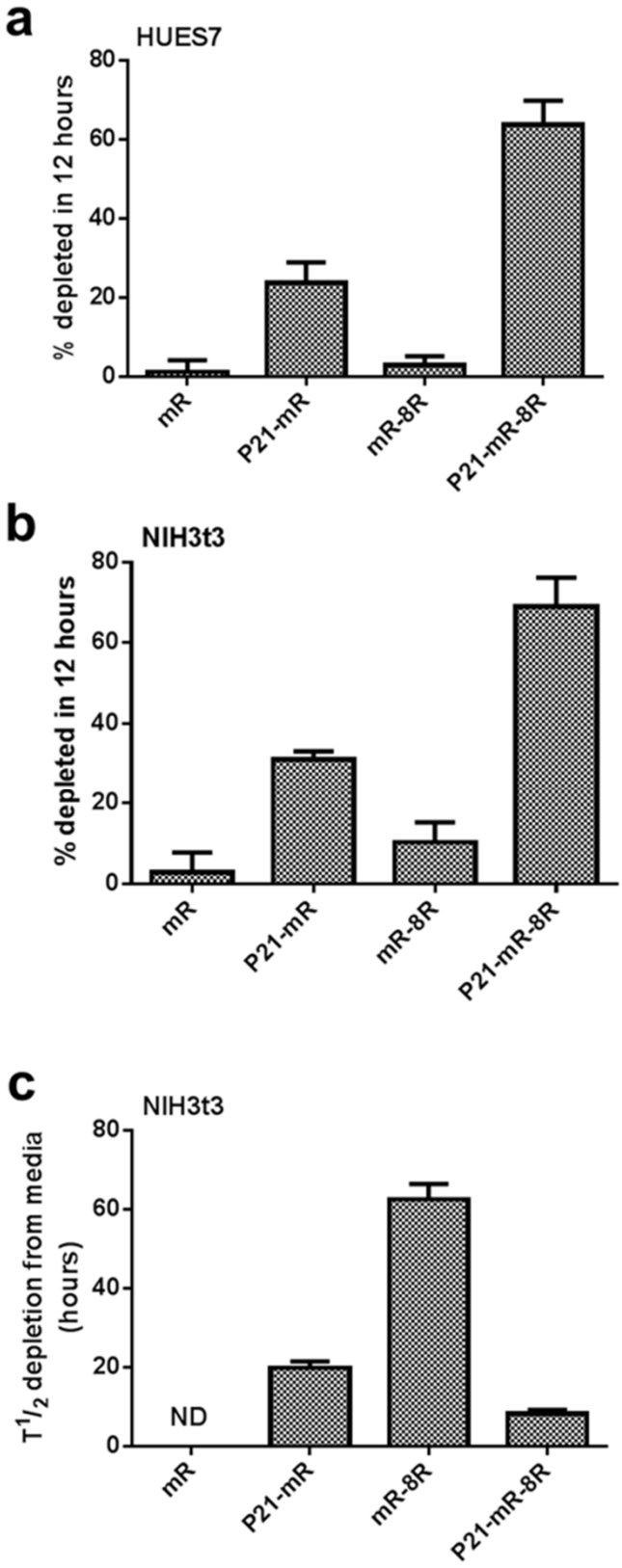
a
HUES7
% depleted in 12 hours
80
60
40
20
0
mR
P21-mR
mR-8R
P21-mR-8R
b
NIH3t3
% depleted in 12 hours
80
60
40
20
0
mR
P21-mR
mR-8R
P21-mR-8R
c
NIH3t3
T1/2 depletion from media (hours)
80
60
40
20
0
ND
mR
P21-mR
mR-8R
P21-mR-8R

Figure S22

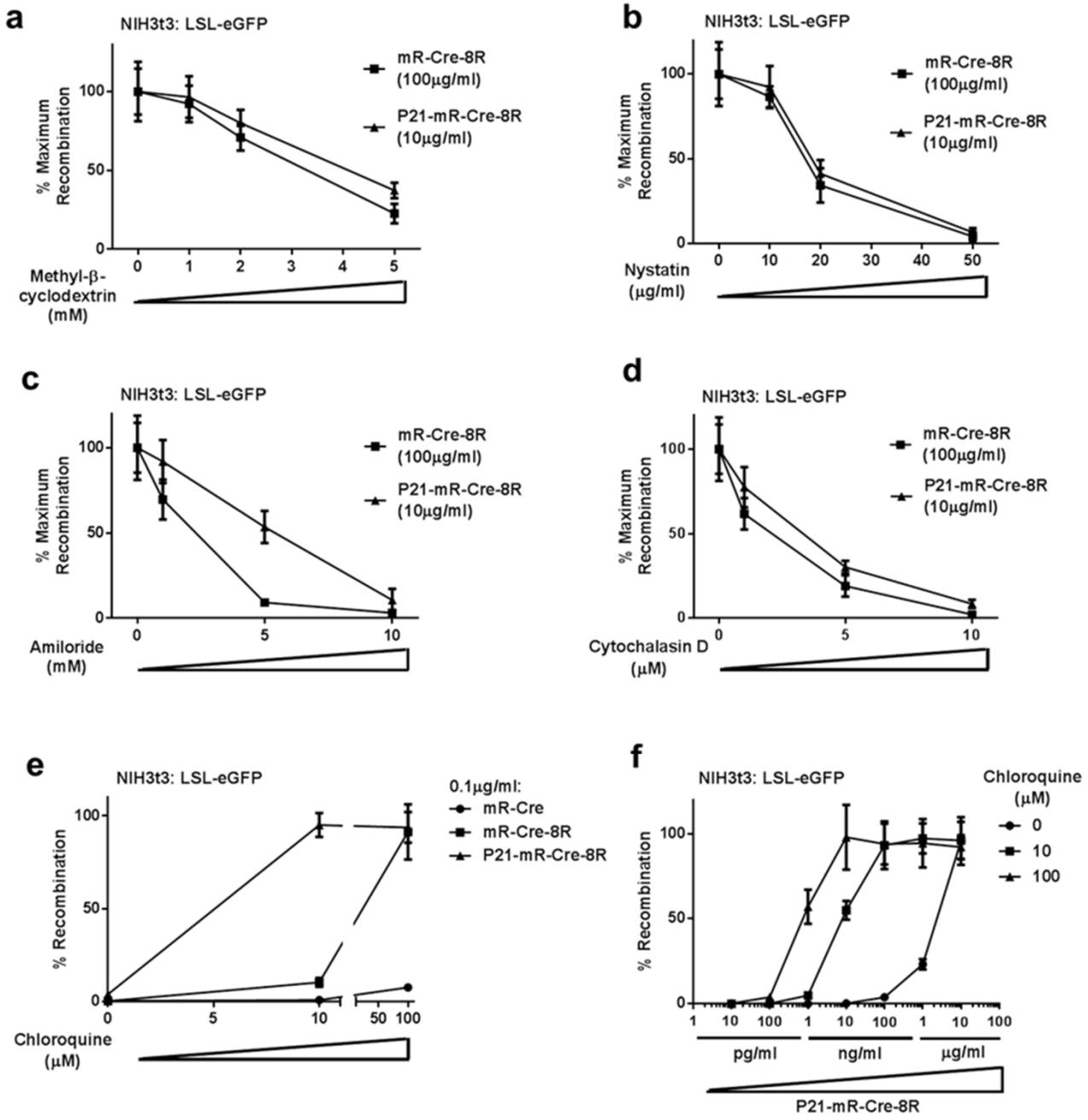
a
NIH3t3: LSL-eGFP
% Maximum Recombination
mR-Cre-8R (100μg/ml)
P21-mR-Cre-8R (10μg/ml)
Methyl-β-cyclodextrin (mM)
b
NIH3t3: LSL-eGFP
% Maximum Recombination
mR-Cre-8R (100μg/ml)
P21-mR-Cre-8R (10μg/ml)
Nystatin (μg/ml)
c
NIH3t3: LSL-eGFP
% Maximum Recombination
mR-Cre-8R (100μg/ml)
P21-mR-Cre-8R (10μg/ml)
Amiloride (mM)
d
NIH3t3: LSL-eGFP
% Maximum Recombination
mR-Cre-8R (100μg/ml)
P21-mR-Cre-8R (10μg/ml)
Cytochalasin D (μM)
e
NIH3t3: LSL-eGFP
% Recombination
0.1μg/ml:
mR-Cre
mR-Cre-8R
P21-mR-Cre-8R
Chloroquine (μM)
f
NIH3t3: LSL-eGFP
% Recombination
Chloroquine (μM)
0
10
100
pg/ml
ng/ml
μg/ml
P21-mR-Cre-8R

Figure S23

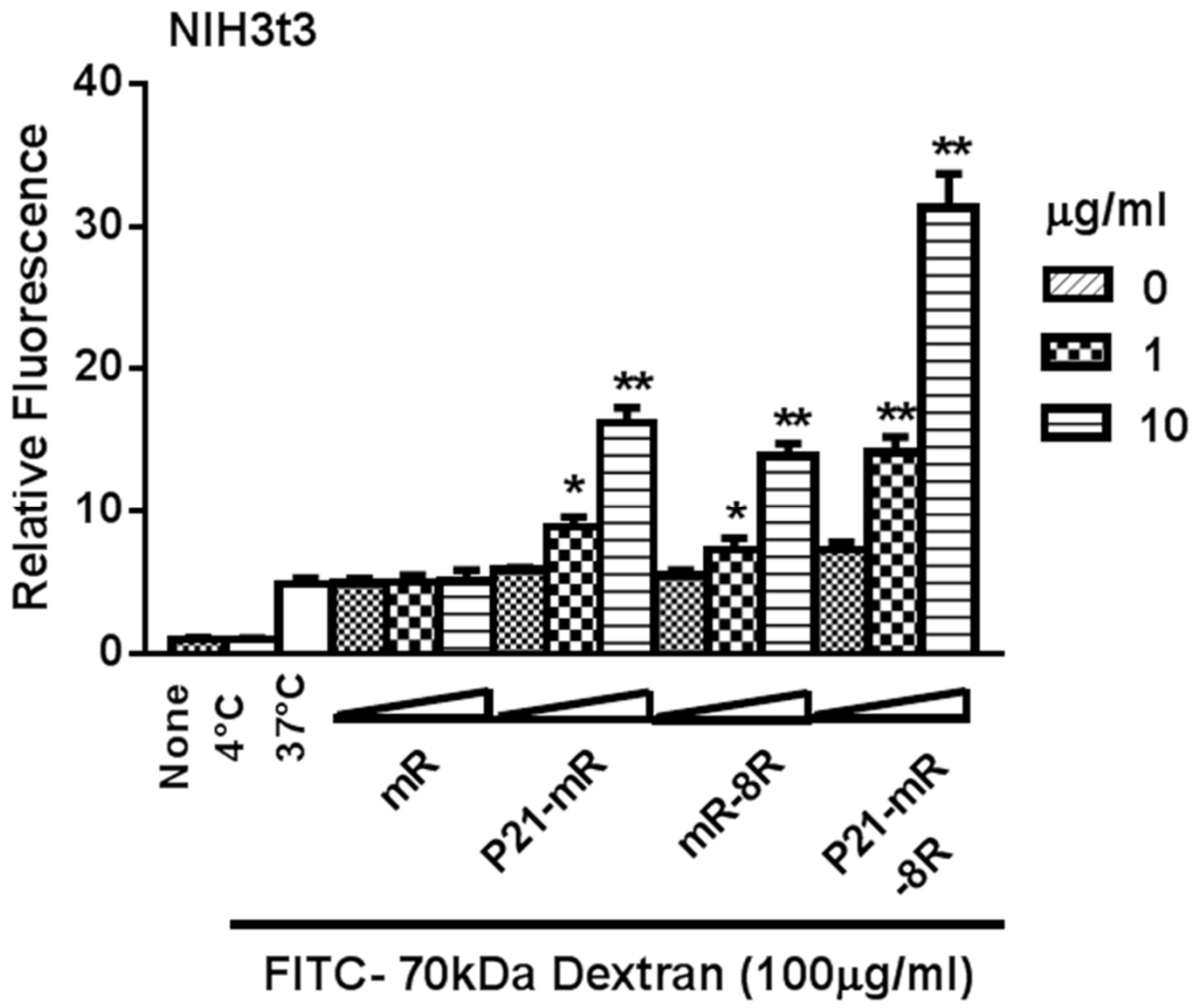
NIH3t3
Relative Fluorescence
40
30
20
10
0
μg/ml
0
1
10
*
**
None
4°C
37°C
mR
P21-mR
mR-8R
P21-mR
-8R
FITC- 70kDa Dextran (100μg/ml)

Figure S24

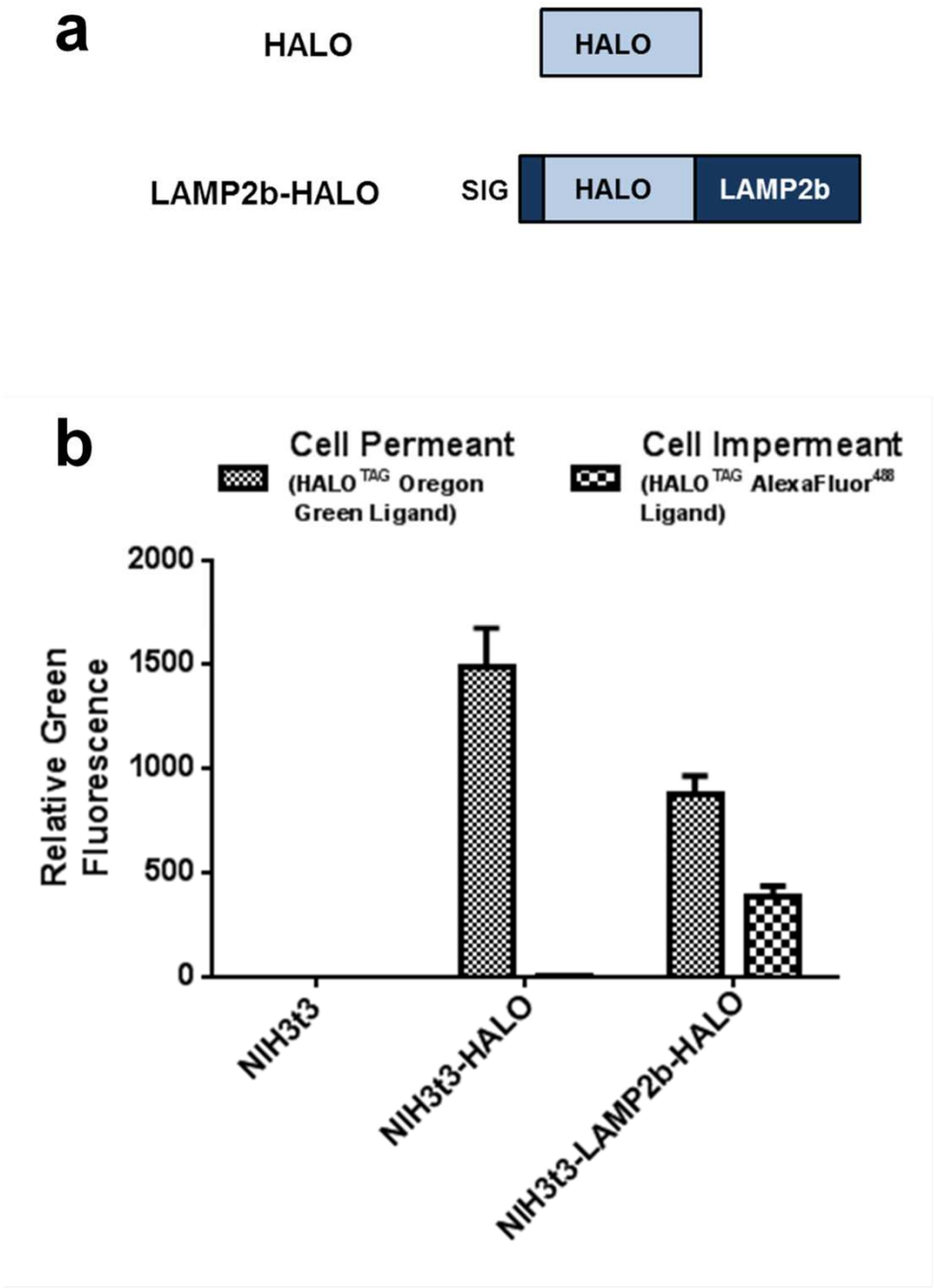
a
HALO
HALO
LAMP2b-HALO
SIG
HALO
LAMP2b
b
Cell Permeant
(HALO TAG Oregon Green Ligand)
Cell Impermeant
(HALO TAG AlexaFluor 488 Ligand)
Relative Green Fluorescence
2000
1500
1000
500
0
NIH3t3
NIH3t3-HALO
NIH3t3-LAMP2b-HALO

Figure S25

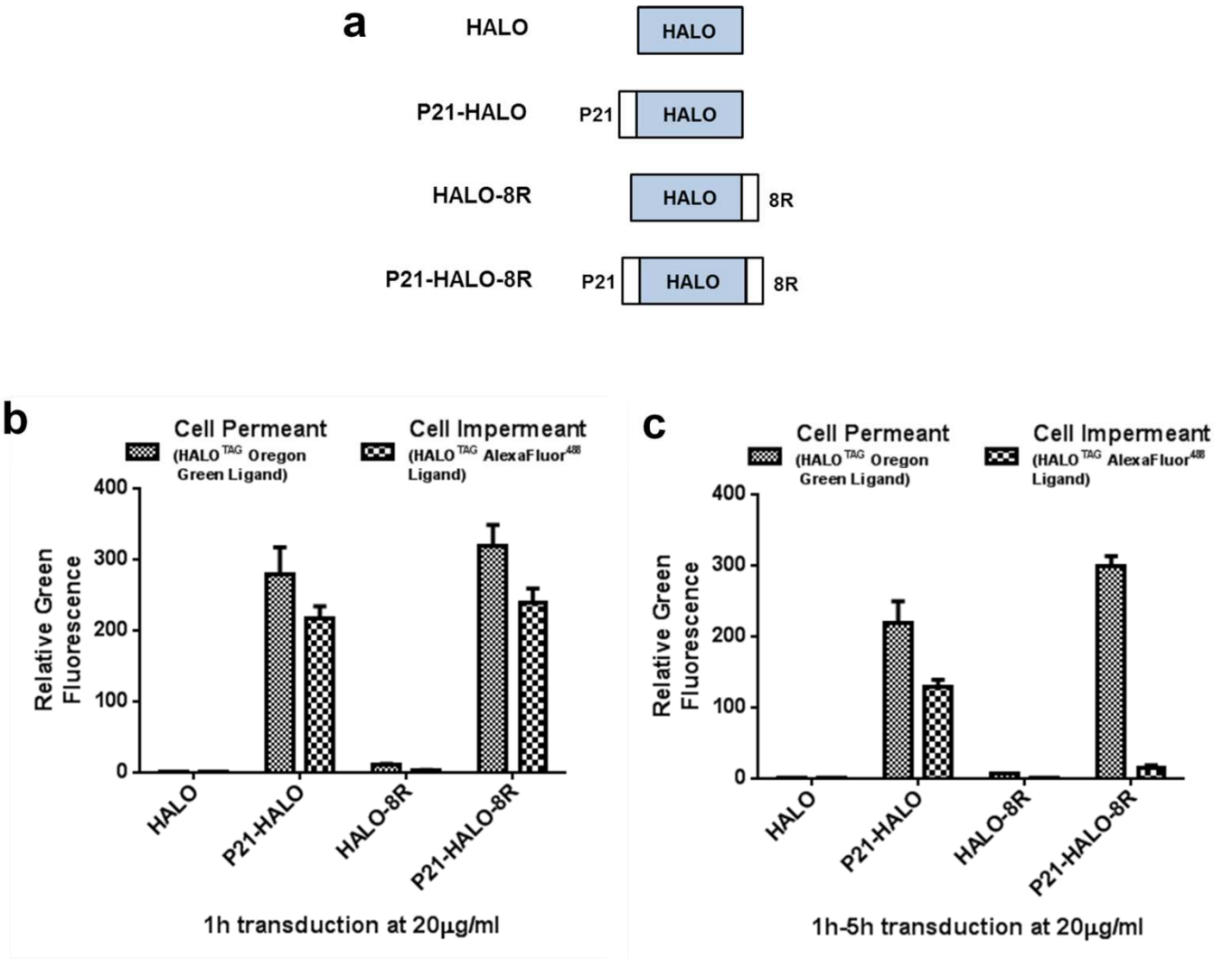
a
HALO
HALO
P21-HALO
P21
HALO
HALO-8R
HALO
8R
P21-HALO-8R
P21
HALO
8R
b
Cell Permeant
(HALO TAG Oregon Green Ligand)
Cell Impermeant
(HALO TAG AlexaFluor 488 Ligand)
Relative Green Fluorescence
400
300
200
100
0
HALO
P21-HALO
HALO-8R
P21-HALO-8R
1h transduction at 20µg/ml
c
Cell Permeant
(HALO TAG Oregon Green Ligand)
Cell Impermeant
(HALO TAG AlexaFluor 488 Ligand)
Relative Green Fluorescence
400
300
200
100
0
HALO
P21-HALO
HALO-8R
P21-HALO-8R
1h-5h transduction at 20µg/ml

Figure S26

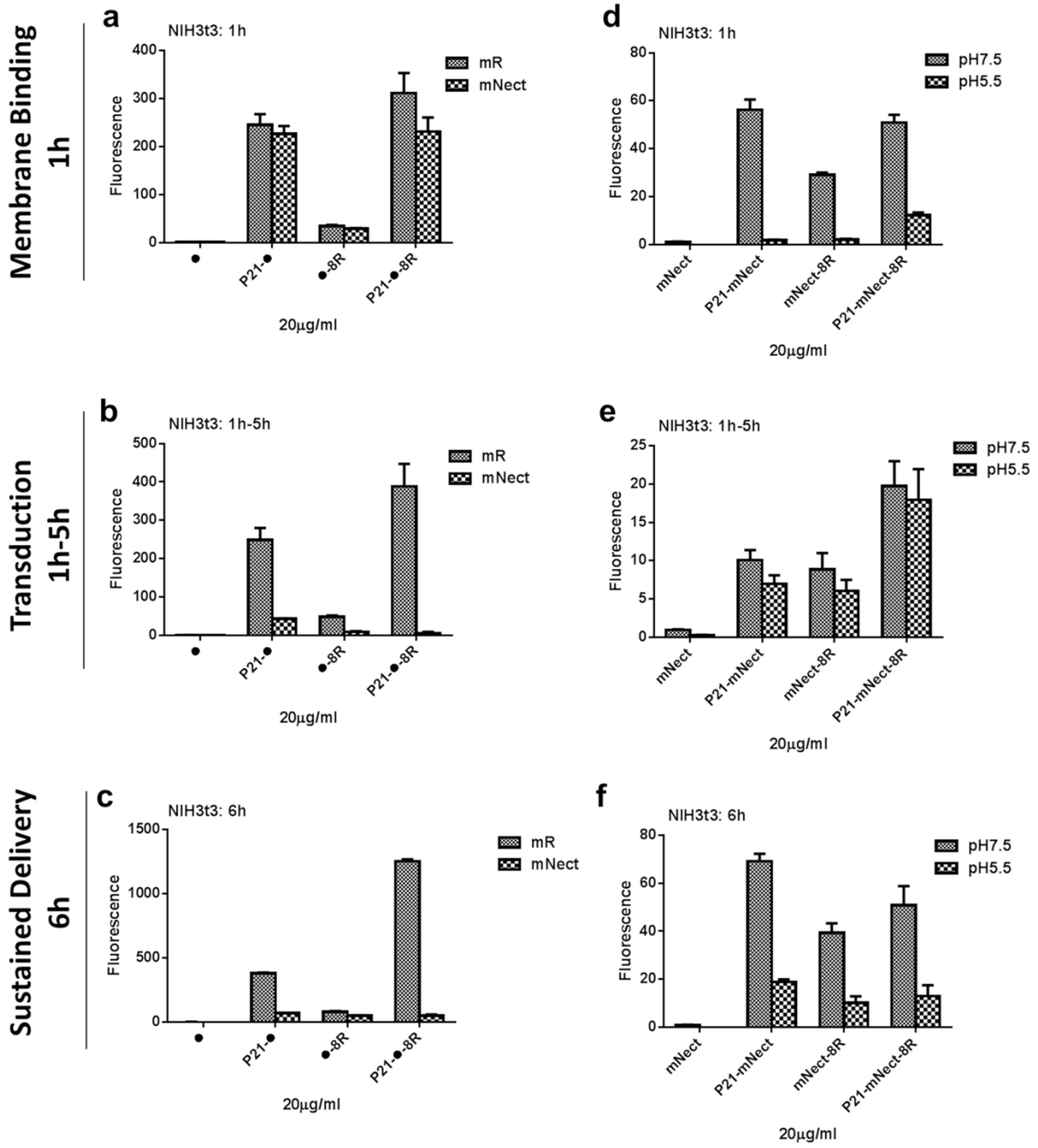
Membrane Binding 1h
Transduction 1h-5h
Sustained Delivery 6h
a
NIH3t3: 1h
Fluorescence
mR
mNect
●
P21-●
●-8R
P21-●-8R
20μg/ml
b
NIH3t3: 1h-5h
c
NIH3t3: 6h
d
NIH3t3: 1h
pH7.5
pH5.5
mNect
P21-mNect
mNect-8R
P21-mNect-8R
e
NIH3t3: 1h-5h
f
NIH3t3: 6h

Figure S27

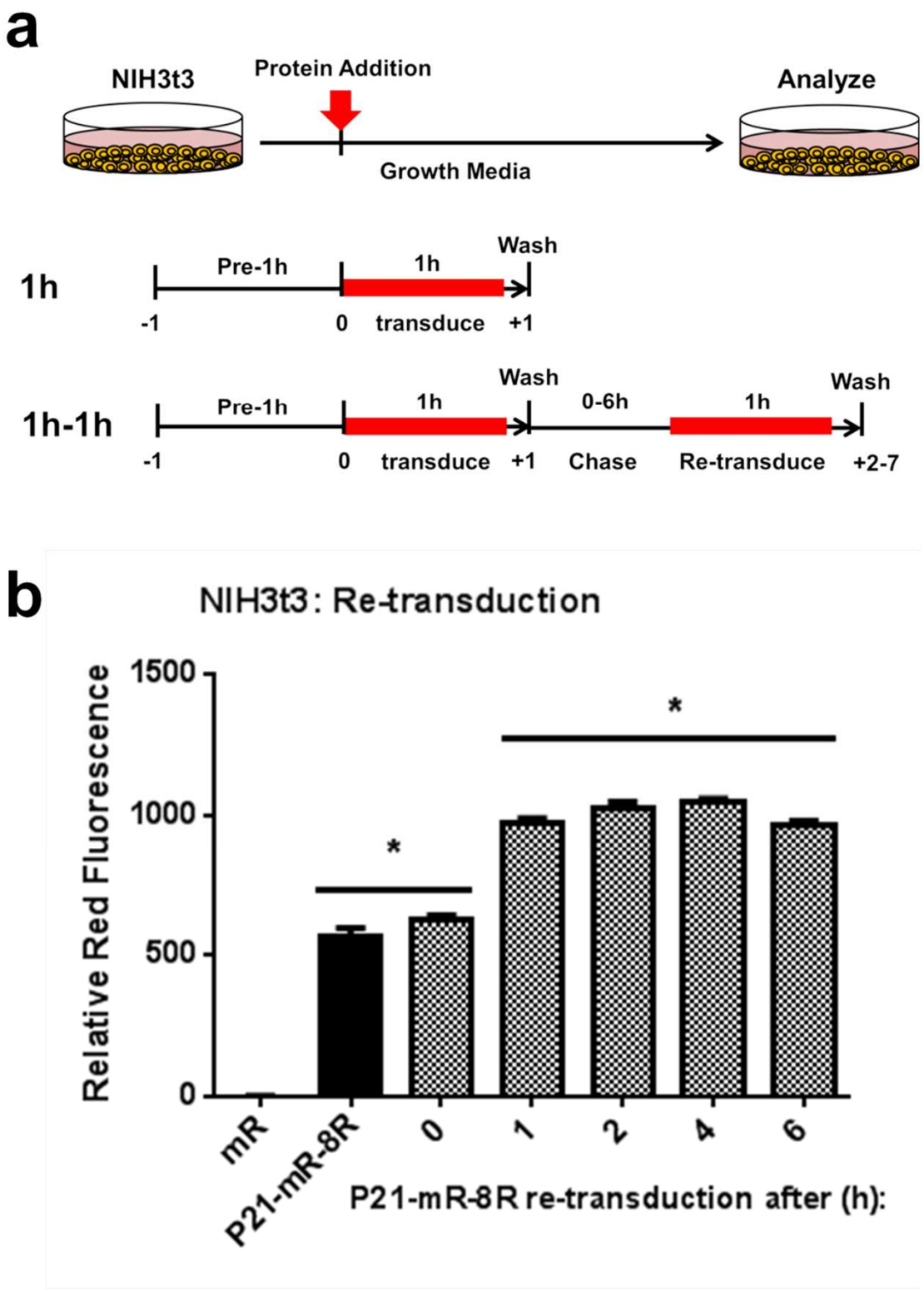
a
NIH3t3
Protein Addition
Analyze
Growth Media
1h
Pre-1h
1h
Wash
-1
0
transduce
+1
1h-1h
Pre-1h
1h
Wash
0-6h
1h
Wash
-1
0
transduce
+1
Chase
Re-transduce
+2-7
b
NIH3t3: Re-transduction
Relative Red Fluorescence
1500
1000
500
0
*
*
mR
P21-mR-8R
0
1
2
4
6
P21-mR-8R re-transduction after (h):

Figure S28

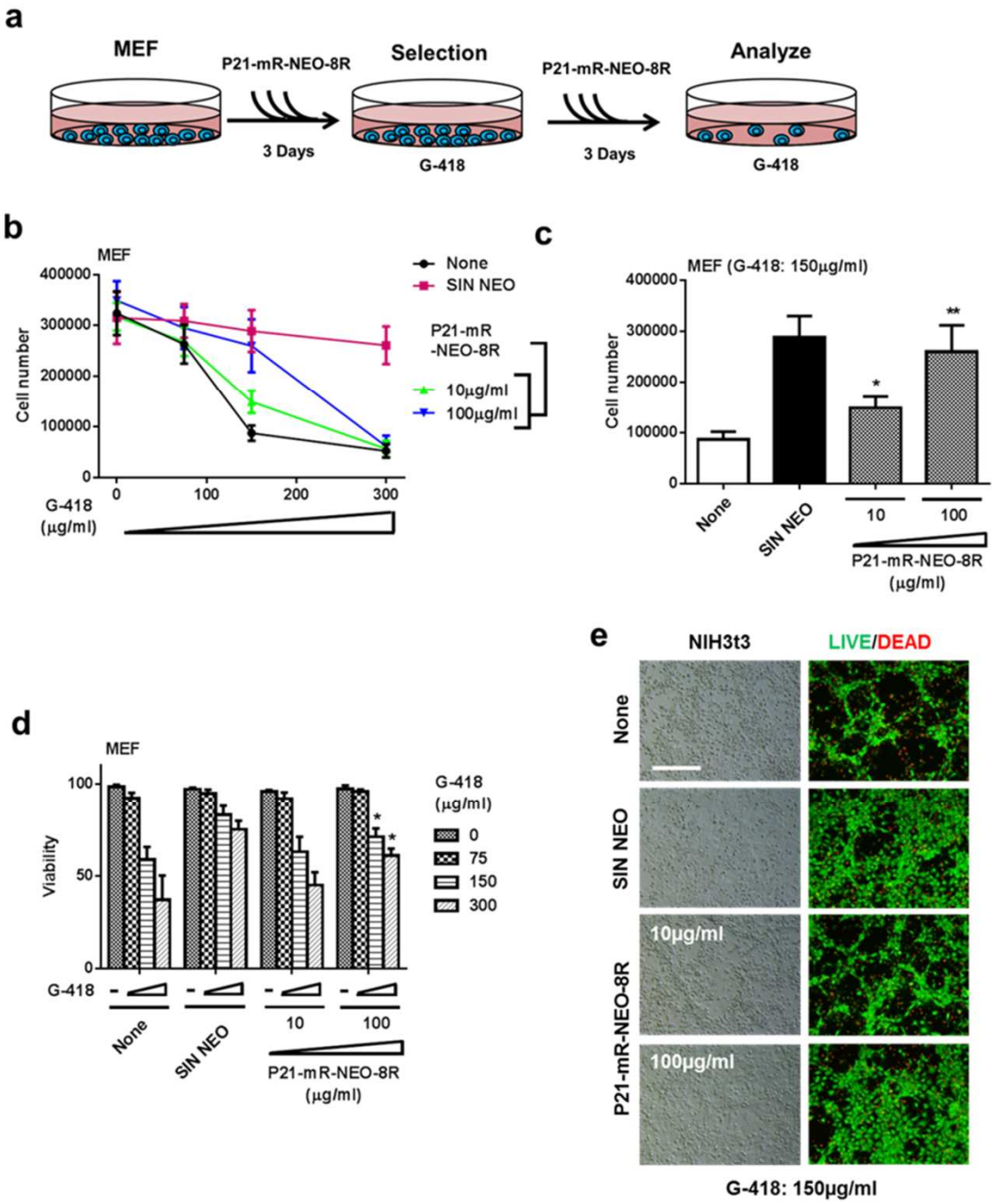
a
MEF
P21-mR-NEO-8R
3 Days
Selection
G-418
P21-mR-NEO-8R
3 Days
Analyze
G-418
b
MEF
Cell number
400000
300000
200000
100000
0
0
100
200
300
G-418
(μg/ml)
None
SIN NEO
P21-mR
-NEO-8R
10μg/ml
100μg/ml
c
MEF (G-418: 150μg/ml)
Cell number
400000
300000
200000
100000
0
*
**
None
SIN NEO
10
100
P21-mR-NEO-8R
(μg/ml)
d
MEF
Viability
100
50
0
G-418
None
SIN NEO
10
100
P21-mR-NEO-8R
(μg/ml)
G-418
(μg/ml)
0
75
150
300
e
NIH3t3
LIVE/DEAD
None
SIN NEO
10μg/ml
P21-mR-NEO-8R
100μg/ml
G-418: 150μg/ml

Table S1

Protein	HBD	Ref Seq	Position	Size	Sequence	Charge at pH7.0
HB-EGF	P21	NP_001936.1	93-113	21	KRKKKGKGLGKKRDPCLRKYK	11
FGF1	FGF1A	NP_000791.1	22-74	53	NYKKPKLLYCSNGGHFLRILPDGTVDGTRDRSDQHIQLQLSAESVGEVYIKST	1.1
	FGF1B	NP_000791.1	111-128	18	TYISKRHAEKNWFVGLKK	4.1
	FGF1C	NP_000791.1	127-144	18	KKNGSCKRGPRTHYGQKA	6
FGF2	FGF2A	NP_001997.5	158-210	53	HFKDPKRLYCKNGGFFLRIHPDGRVDGVREKSDPHIKLQLQAEERGVVSIKGV	4.2
	FGF2B	NP_001997.5	247-262	16	TYRSRKYTSWYVALKR	5
	FGF2C	NP_001997.5	261-278	18	KRTGQYKLGSKTGPGQKA	5
FGF4	FGF4A	NP_001998.1	80-131	52	IKRLRRLYCNVGIGFHLQALPDGRIGGAHADTRDSLLELSPVERGVVSIFGV	2.1
	FGF4B	NP_001998.1	168-183	16	AYESVKYPGMFIALSK	1
	FGF4C	NP_001998.1	182-199	18	SKNGKTKKGNRVSPTMKV	6
FGF7	FGF7A	NP_002000.1	62-113	52	GDIRVRRLFCRTQWYLRIDKRGKVKGTQEMKNNYNIMEIKTVAVGIVAIKGV	8
	FGF7B	NP_002000.1	150-169	20	TYASAFWTHNGGEMFVALNQ	0.1
	FGF7C	NP_002000.1	168-185	18	NQKGIPVRGKKTKKEQKT	6
BMP2	BMP2	NP_001191.1	283-299	17	QAKHKQRKRLKSSCKRH	8.1
BMP4	BMP4	NP_001193.2	293-311	19	SPHHHSQRARKKNKNCRRH	16.4
BMP7	BMP7	NP_001710.1	293-333	41	STQSKQRSQNRSKTPKNQEALRMANVAENSSSDQRQACKKH	6
LTBP-1L	TGFBP	NP_996826.2	1339-1412	73	DQPKEEKKECYVNLNDASLCDNVLAPNVTKQECCTSGAGWGDNCEIFPCPVLGTAEFTEMCPKGKFVPAGE	-6.3
NOGGIN	NOG	NP_005441.1	131-146	16	QGKKQRLSKKLRRKLQ	7
Antithrombin-III	ATIII	NP_000479.1	108-129	22	AKLNCRLYRKANKSSKLVSANR	7
PDGF	PDGF	NP_002598.4	194-211	18	GRPRESGKKRKRKRRLKPT	9
VEGF	VEGF	NP_001165095.1	166-215	50	PCGPCSERRKHLFVQDPQTCKCSCRNTDSRCKARQLELNERTCRCDKPRR	6.7
Fibronectin	FN	NP_997643.1	1721-1991	271	AIPAPTDLKFTQVTPTSLSAQWTPPNVQLTGYRVRVTPKEKTGPMKEINLAPDSSSVVVSGLMVATKYEVSVYALKDTLTSRPAQGVVTLENVSPPRRA RVTDATETTITISWRTKTETITGFQVDAVPANGQTPIQRTIKPDVRSYTITGLQPGTDYKIYLYTLNDNARSSPVVIDASTAIDAPSNLRFLATTPNSLL VSWQPPRARITGYIIKYEKPGSPPREVVPRPRPGVTEATITGLEPGTEYTIYVIALKNNQKSEPLIGRKKT	10
Fibrinogen	FBN	NP_005132.2	61-95	36	PAPPPISGGGYRARPAKAAATQKKVERKAPDAGGC	5
Fibrillin-1	Fib1 TB5	NP_000129.3	1689-1765	77	DMRRSLCYRNYYADNQTCDGELLFNMTKKMCCSYNIGRAWNKPCEQCPIPSTDEFATLCGSQRPGFVIDIYTGLPV	-0.4

Supplemental Figure Legends

Figure S1 Inefficient Protein Delivery in Pluripotent Cells. **(a)** Schematic of the proteins created to determine the efficiency of protein delivery. mR is mRFP only as a poorly transducing control protein representing background uptake. mR-8R is mRFP with a C-terminal fusion of eight Arginine residues (8R) to promote transduction. **(b)** mR-8R is taken up efficiently into NIH3t3 cells. Fluorescence microscopy images of NIH3t3 cells treated with mR or mR-8R (100µg/ml) for twelve hours in standard media conditions. Scale bar, 100µm. **(c)** mR-8R is taken up inefficiently into human and mouse embryonic stem cells (HUES7 and CGR-8, respectively), human induced pluripotent stem cells (IPS2) and mouse cardiomyocyte cell line HL1. Fluorescence microscopy images of multiple cell lines treated with mR-8R (100µg/ml) for twelve hours in cell-type specific media conditions. Scale bar, 100µm. **(d)** Flow cytometry analyses of the multiple cell lines treated with different dosages of mR-8R (0, 1, 5, 10, 20, 50 and 100µg/ml) for twenty-four hours. **(e)** Flow cytometry analyses of the 100µg/ml dose for twenty-four hours. Graphs show relative fluorescence units (R.F.U.). Error bars indicate s.d. n=6.

Figure S2 PTD-proteins bind to Pluripotent cells but are taken up poorly. Fluorometry of media to determine the remaining fluorescent protein remaining after incubation with cells. mR-8R was diluted to 20µg/ml in serum-free media and 1ml/well incubated for either 1 hour **(a)** or 12 hours **(b)** with confluent NIH3t3, MEF, CGR-8, HUES7 or IPS2 cells in 6 well plates. Fluorescence pre-incubation was assigned as 100% of units and background of serum-free media subtracted. Error bars indicate s.d. n=6.

Figure S3 P21 binds directly to heparin. Fluorometry to determine the fluorescent protein remaining after incubation with heparin-sepharose beads. Recombinant proteins were diluted (20µg/ml) in serum-free media and 1ml/tube incubated for 1 hour at 37˚C with 50µl heparin-sepharose with rotation. Fluorescence pre-incubation was assigned as 100% of units and background of serum-free media subtracted. Error bars indicate s.d. n=6.

Figure S4 GET of domain position protein variants. **(a)** Schematic of the proteins created to test the effect of domain position on protein delivery to cells. **(b)** Fusion of P21 and 8R to mR in any orientation significantly improves transduction. Flow cytometry analyses of NIH3t3 and HUES7 cells incubated with the protein variants (20µg/ml) for twelve hours. Error bars indicate s.d. n=6.

Figure S5 GET of PTD protein variants. **(a)** Schematic of the proteins created to test the enhancing effect of P21 on other PTDs for protein delivery to cells. 8R is RRRRRRRR, TAT is HIV-1 TAT protein RKKRRQRRR, 8K is KKKKKKKK, 8RQ is RQRQRQRQ **(b)** Fusion of P21 and any PTD to mR significantly improves transduction. Flow cytometry analyses of NIH3t3 and HUES7 cells incubated with the protein variants (20µg/ml) for twelve hours. Error bars indicate s.d. n=6.

Figure S6 P21 sequence not charge is required for optimal cellular uptake. (a) Schematic of the proteins created to assess the sequence requirements for improved efficiency of protein delivery to cells. mR and P21-mR-8R are described in Fig 1. P21*-mR-8R contains a scrambled P21 sequence. P21 KR only-mR-8R contains only the positive residues from P21.

The sequences are shown. **(b)** The intact P21 sequence is required to synergise with PTD for enhanced delivery. NIH3t3 cells were treated with proteins (20µg/ml) for twelve hours in standard media conditions. mRFP-24R is shown as an equivalent positively-charged protein. **(c)** P21 enhances super-charged protein uptake into cells. mRFP was fused to 4, 8, 16, 24, 32 and 48 arginines (R) with or without P21 fusion. NIH3t3 cells were treated with proteins (20µg/ml) for twelve hours. **(d)** P21 activity is not mediated by positive-charging. Data from c) was represented plotted against the theoretical protein charge (at pH 7.0). P21-tagged proteins requires an overall positive charge of ~+20 for maximal transduction. Error bars indicate s.d. n=6.

Figure S7 GET is reproducible for other growth-factor and extracellular matrix HBDs and PTDs. (a) Schematic of the proteins created to assess the effect of other natural HBDs on the uptake of proteins with PTDs. HBDs were cloned replacing the P21 sequence. (b) HBDs enhance PTD-mediated transduction with different efficacy. P21 was compared to HBDs from the FGF (FGF1, 2, 4 and 7, 3 HBDs each, A, B or C), BMP (BMP2, 4 and 7), TGFβ-regulators (LTBP1 and Noggin), antithrombin (ATIII), PDGF and VEGF growth factor families and extracellular matrix protein HBDs (Fibronectin, FN; Fibrinogen, FBN; and Fibrillin; Fib1 TB5) when fused to mR or mR-8R. NIH3t3 cells were treated with proteins (20µg/ml) for twelve hours. (c) HBDs have cell-type specific enhancement of PTDs. NIH3t3 cells were compared with transduction with CGR8 and HUES7 cells for the FGF family HBDs, ATIII, PDGF and VEGF. (d) HBD-mediated enhancement is not dependent on positive charge. Data from b) was represented plotted against the theoretical protein charge (at pH 7.0). Error bars indicate s.d. n=6.

Figure S8 P21 binds directly to heparin and cell surface heparin sulfate-GAG. **(a)** Soluble heparin in media during transduction inhibits cell membrane interaction and uptake of P21-containing proteins. Fluorescence microscopy images of CGR-8 cells treated with P21-mR-8R (20µg/ml) for 6 hours in serum-free media containing 0 or 50µg/ml Heparin. Scale bar, 100µm. **(b)** Flow cytometry analyses NIH3t3 cells treated with P21-mR-8R (20µg/ml) for 6 hours with or without a variety of GAGs (50µg/ml) in serum-free medium. CS is Chondroitin sulfate. Cells were pre-incubated for 1 hour in serum-free media and incubated for 6 hours in serum-free media with or without GAGs. **(c-d)** Only high-doses of Heparin inhibit 8R activity whereas P21 activity is inhibited dose-dependently by Heparin in **(c)** NIH3t3 cells and **(d)** CGR-8 cells. **(e-f)** Cell surface Heparan sulfate is required for efficient P21-mediated protein delivery. Heparan sulfates/Heparin-containing FCS inhibits P21-mediated uptake but can also replace cell surface GAGs and mediate P21-uptake in cells deficient for Heparan sulfate. Fluorescence microscopy images of CGR-8 cells and *EXT1-/-* mESCs treated with P21-mR-8R (20µg/ml) for 6 hours in media containing 0 or 20% FCS. Scale bar, 100µm. Error bars indicate s.d. n=6.

Figure S9 PTD-mediated delivery is inhibited by free heparin and chondroitin sulfate. Flow cytometry analyses NIH3t3 cells treated with mR-8R (20µg/ml) for 6 hours with or without a variety of GAGs (50µg/ml) in serum-free medium. CS is chondroitin sulfate. Cells were pre-incubated for 1 hour in serum-free media and incubated for 6 hours in serum-free media with or without GAGs. Error bars indicate s.d. n=6.

Figure S10 GET is inhibited by GAG-containing FCS, heparinase treatment and competing soluble heparin. **(a-b)** Flow cytometry of transduced cells pre-treated with heparinase. **(a)**

NIH3t3 cells were pre-incubated in serum-free media for 1 hour with different amounts of heparinase III (0, 0.01, 0.1 or 1 U/ml) and incubated with mR or P21-mR-8R (20µg/ml in serum-free media) containing heparinase III for 12 hours. **(b)** NIH3t3 cells were pre-incubated in serum-free media for 1 hour with different amounts of heparinase III and incubated with P21-mR-8R (20µg/ml) containing heparinase III and different amounts of FCS (0, 1 or 10% (v/v)) for 12 hours. **(c)** Flow cytometry of NIH3t3 cells incubated in different concentrations of FCS or FCS which has been depleted for P21-binding material. NIH3t3 cells were pre-incubated in serum-free media for 1 hour and transduced with P21-mR-8R (20µg/ml) containing different amounts of FCS (0, 0.1, 0.5, 1, 2, 5, 10 or 20 (v/v)) for 6 hours. **(d)** Flow cytometry of NIH3t3 cells transduced in 10% FCS or 10% P21 binder-depleted FCS with the addition of soluble heparin. NIH3t3 cells were pre-incubated in serum-free media for 1 hour and incubated with P21-mR-8R (20µg/ml) containing either type of FCS and different amounts of soluble heparin (0, 0.1, 0.5, 1, 2, 5 or 50 µg/ml) for 6 hours. Error bars indicate s.d. n=6.

Figure S11 GET is inhibited by HS-GAG synthesis inhibitor sodium chlorate. Flow cytometry analyses NIH3t3 cells treated with P21-mR-8R (20µg/ml) for 6 hours with or without sodium chlorate (SC, 20mM) in serum-free medium. Cells were pre-incubated with or without SC for 1 hour in serum-free media and incubated for 6 hours in serum-free media with or without SC. Error bars indicate s.d. n=6.

Figure S12 GET compared to CPP-only transduction of NANOG. **(a)** Schematic of the mR-NANOG-8R (CPP-only protein) and P21-mR-NANOG-8R (GET protein). **(b)** P21-mR-NANOG-8R maintains the proliferation of mESCs lacking LIF dose dependently whereas mR-NANOG-8R has poor self-renewal activity. Data shows the percentage of the number of CGR-8 cells cultured without LIF verses those with LIF (% -LIF/+LIF) at passaging. In LIF-deficient CGR-8 cultures proliferation is promoted when supplemented with SIN NANOG (to overexpress NANOG) or transduced with P21-mR-NANOG-8R but poorly by mR-NANOG-8R. Error bars indicate s.d. n=6.

Figure S13 GET compared to CPP-only transduction of MYOD. **(a)** Schematic of the mR-MYOD-8R (CPP-only protein) and P21-mR-MYOD-8R (GET protein). **(b)** P21-mR-MYOD-8R drives myogenic differentiation of HUES7 cells to MYOGENIN positive multinucleated Myotubes whereas mR-MYOD-8R has poor myogenic activity. P21-mR-MYOD-8R activity is comparable to cells genetically supplemented with SIN MYOD (to overexpress MYOD). Data shows the quantitation of the percentage MYOGENIN positive cells using immunolabelling. Error bars indicate s.d. n=6.

Figure S14 Delivery of a tissue-extracted pro-apoptotic protein by GET-mSA2. **(a)** Schematic of bovine heart cytochrome-C (Cyt-C) and biotinylated Cyt-C (BIO-Cyt-C) and Cyt-C complexes with mSA2. **(b)** Co-incubation of Cyt-C (as a non-interacting control) or BIO-Cyt-C (10µg/ml) with GET-mSA2 proteins in the presence of Chloroquine (100µM) to induce apoptosis of NIH3t3s. As assessed by trypan blue exclusion after a 12 hour incubation only the fully interacting and transducing complex (with Chloroquine) mediated loss of cell viability. Error bars indicate s.d. n=6. **(c)** BIO-Cyt-C transduced with P21-mSA2-8R in the

presence of chloroquine caused complete loss of cell viability demonstrated by light microscopy. (scale bar, 50µm).

Figure S15 GET of Antibodies using SpA B domain. **(a)** Schematic of the SpAB and P21-SpAB-8R proteins engineered to bind to and transduce IgG antibodies. We tested the delivery of an FITC-conjugated Rabbit anti-mouse IgG (Rb IgG-FITC). **(b)** IgG (1µg/ml) was taken into NIH3t3 cells poorly by direct incubation or when co-incubated with SpAB (left panel). With co-incubation of P21-SpAB-8R (10µg/ml, right panel), IgG was efficiency delivered to cells visible by fluorescence microscopy (scale bar, 50µm). **(c)** Flow cytometry of delivered cells confirmed an increase in IgG delivery of over 2-orders of magnitude. Error bars indicate s.d. n=6.

Figure S16 GET compared to CPP-only transduction of NEO. **(a)** Schematic of the mR-NEO-8R (CPP-only protein) and P21-mR-NEO-8R (GET protein). **(b)** P21-mR-NEO-8R maintains living cultures of MEFs under G-418 selection whereas mR-NEO-8R has poor rescue activity. P21-mR-NEO-8R activity is comparable to cells genetically supplemented with SIN NEO (to overexpress NEO). Data shows MEF cell numbers for the 150µg/ml dose of G-418. Error bars indicate s.d. n=6.

Figure S17 P21 and CPP addition to cargoes improves delivery by > two-orders of magnitude. Cell lines (described in Fig. 1) including rat aortic smooth muscle cells (rSMC) and neonatal cardiomyocytes (rCMs) were transduced with mRFP fused-variants of cargo proteins (mR, mR-Cre, mR-NEO, mR-NANOG or mR-MYOD) or with cargoes with N-

terminally fused P21 and C-terminally fused 8R (CPP) sequences (GET proteins; P21-mR-8R, P21-mR-Cre-8R, P21-mR-NEO-8R, P21-mR-NANOG-8R or P21-mR-MYOD-8R). Incubations were at 20µg/ml protein for 24 hours in the cell-line standard media. Data shows the fold increase of uptake with addition of GET sequences (P21 and 8R) to the cargoes as assessed by flow cytometry. Error bars indicate s.d. n=6.

Figure S18 High level or constant GET-uptake does not affect cell viability **(a)** Assessment of cell viability by trypan blue exclusion of NIH3t3s incubated for 12 hours with 0-200 µg/ml P21-mR-8R protein either directly after incubation (0h; left) or 24 hours-post incubation (24h; right). **(b)** Assessment of cell proliferation after incubation by passaging and cell counts of NIH3t3s incubated for 24 hours with 0-200 µg/ml P21-mR-8R protein. **(c)** Assessment of cell proliferation during constant incubation by passaging and cell counts of NIH3t3s incubated with 0-200 µg/ml P21-mR-8R protein (protein refreshed at each passage). Cells were passaged daily and re-plated at 100,000 cells per 12 well. Error bars indicate s.d. n=6.

Figure S19 GET is biocompatible in multiple clinically relevant cell types. Cell lines were incubated with P21-mR-8R at 20 or 200µg/ml over 24 hours and assessed by trypan blue for cell viability (cell lines were those described in Fig. 1 including rat aortic smooth muscle cells (rSMC) and neonatal cardiomyocytes (rCMs)). Viability remained high in all cell types for both concentrations tested. Error bars indicate s.d. n=6.

Figure S20 GET can achieve higher intracellular levels of cargo delivery than transgenic systems. **(a)** Fluorometry of soluble extracts generated from NIH3t3 mR (transgenic NIH3t3

cells transduced with SIN mR) compared with those from NIH3t3 cells incubated for 6 hours with different doses of mR-8R or P21-mR-8R (0, 10, 20, 50, 100 or 200µg/ml in serum-free media) **(b)** Flow cytometry of NIH3t3 mR (transgenic NIH3t3 cells transduced with SIN mR) compared with those from NIH3t3 cells transduced for 6 hours with different doses of mR-8R or P21-mR-8R (0, 10, 20, 50, 100 or 200µg/ml in serum-free media). Fluorescence is normalised to untreated NIH3t3 cells. Error bars indicate s.d. n=6.

Figure S21 GET proteins are rapidly depleted from culture media by efficient cellular uptake. **(a-b)** Fluorometry of media to determine the remaining fluorescent protein remaining after incubation with cells. Recombinant proteins were diluted to 20µg/ml in serum-free media and 1ml/well incubated for 12 hours with confluent NIH3t3s in 6 well plates. Fluorescence pre-incubation was assigned as 100% of units and background of serum-free media subtracted. **(a)** HUES7-mediated depletion of recombinant proteins from culture media in 12 hours. **(b)** NIH3t3-mediated depletion of recombinant proteins from culture media in 12 hours. **(c)** The $T_{1/2}$ depletion was calculated by incubating NIH3t3 cells with recombinant proteins (20µg/ml) for different times. Bar chart shows the time (hours) required to deplete the recombinant protein to half the starting concentration in the described system. Error bars indicate s.d. n=6.

Figure S22 Cre Recombinase nuclear activity is promoted by vesicle escape but repressed by inhibitors of macropinocytosis or cholesterol depletion by GET. NIH3t3: LSL-eGFP cells were pre-incubated in serum-free media (with or without drugs), transduced with Cre proteins (mR-Cre: 100µg/ml or P21-mR-8R: 10µg/ml) for 1 hour in serum-free media (with or without drugs), washed and cultured for 12 hours in full growth media (with or without

drugs) and a further 36 hours in full growth media before analyses. **(a)** Methyl-β-cyclodextrin (used to deplete cholesterol) inhibits Cre transduction and recombination. (Methyl-β-cyclodextrin doses were 0, 1 2 and 5 mM). **(b)** Nystatin (a drug which sequesters cholesterol) inhibits Cre transduction and recombination. (Nystatin doses were 0, 10, 20 and 50µg/ml). **(c)** Amiloride (a specific inhibitor of Na^+/H^+ exchanged required for macropinocytosis) inhibits Cre transduction and recombination. (Amiloride doses were 0, 1, 5 or 10mM). **(d)** Cytochalasin D (an F-actin elongation inhibitor) inhibits Cre transduction and recombination. (Cytochalasin D doses were 0, 1, 5 or 10µM). **(e)** Chloroquine promotes the release of Cre from endosomal vesicles and increases recombination (Chloroquine doses were 0, 10 and 100µM). **(f)** Picogram per millilitre amounts is required to induce recombination with enhanced vesicle escape. The dose of transduced P21-mR-Cre-8R was varied in ten-fold dilutions (0-100µg/ml) with 1 hour incubation in the presence of Chloroquine. All data is presented as % of the maximal recombination. Error bars indicate s.d. n=6.

Figure S23 GET increases general cellular macropinocytosis. Flow cytometry of cells incubated in 70kDa FITC-Dextran and transduced with recombinant proteins. NIH3t3 cells were pre-incubated in serum-free media for 1 hour and transduced with mR, P21-mR, mR-8R or P21-mR-8R (20µg/ml in serum-free media) containing 70kDa FITC-Dextran (neutral) for 1 hour. Error bars indicate s.d. n=6.

Figure S24 Ligand auto-labelling of intracellular and extracellular membrane-anchored HALO proteins. **(a)** Schematic of the HALO (intracellular) and LAMP2b-HALO (extracellular membrane-anchored) transgenic SIN lentivirus constructs. In LAMP2b-HALO the expressed protein is localised to the cell membrane by the signal peptide (SIG) which is

cleaved and presented on the extracellular side of the cell membrane **(b)** NIH3t3 cells transgenic for intracellular HALO protein (NIH3t3-HALO) are only efficiently labelled by cell permeant ligands ($HALO^{TAG}$ Oregon Green). NIH3t3 cells transgenic for membrane-anchored extracellular HALO protein (NIH3t3-LAMP2b) is efficiently labelled by both cell permeant and cell impermeant ligands ($HALO^{TAG}$ $Alexafluor^{488}$). Data shows flow cytometry of the NIH3t3 cell-lines incubated in ligand (1µM) for 15mins, followed by 3 media washes and a 15mins incubation to remove unbound ligand. Error bars indicate s.d. n=6.

Figure S25 Ligand labelling of GET-HALO proteins demonstrates rapid cell binding and uptake. **(a)** Schematic of HALO proteins created (as described for mRFP in fig 1). **(b)** P21-HALO-8R and P21-HALO efficiently bind NIH3t3 cells but do not significantly internalise with a 1 hour incubation. **(c)** Bound P21-HALO-8R efficiently is taken into NIH3t3 cells with further incubation (1h-5h). Bound P21-HALO does not as efficiently enter cells and remains bound to cell membrane with further incubation. Data shows flow cytometry analyses of NIH3t3 cells treated with proteins (20µg/ml) for 1 hour followed direct ligand labelling (1h) or further incubation of 5 hours (1h-5h). Error bars indicate s.d. n=6.

Figure S26 pH-sensitivity of GET-mNectarine (mNect) proteins demonstrates rapid cell binding and uptake. **(a)** Schematic of HALO proteins created (as described for mRFP in fig 1). **(b-c)** GET-mNect or GET-mR proteins (20µg/ml) were transduced into NIH3t3 cells for 1h (to demonstrate membrane binding activity), 1h followed by a further 5h incubation without protein (1h-5h) (to demonstrate transduction activity) or 6h (to demonstrate sustained delivery). Flow cytometry was used to compare intensities of mNect and mR GET-proteins. Fluorescence signal from mNect proteins (unlike mR versions) is rapidly lost after

internalisation new to endosomal acidification and protein unfolding. Error bars indicate s.d. **(d-f)** GET-mNect proteins (20µg/ml) were delivered into NIH3t3 cells for the same regimes but washed in DMEM at pH7.5 or pH5.5 before cytometry. Membrane localised mNect protein fluorescence is extinguished by pH5.5 but is retained at pH7.5 indicating at 1h incubations leave P21-mNect-8R external to cells, bound to membranes and not protected from pH-mediated unfolding. 1h-5h incubations demonstrate that P21-mNect-8R localisation is shifted and protected from pH-mediated unfolding demonstrating internalisation of the protein and protection by the cell membrane. Error bars indicate s.d. n=6.

Figure S27 GET protein must be delivered intracellularly to allow successful re-delivery **(a)** Scheme of testing the effect of re-transduction of GET proteins in NIH3t3 cells. Cells were pre-incubated in fresh media for 1 hour and transduced with P21-mR-8R (20µg/ml) for 1 hour. Cells were then either analysed for fluorescence or re-delivered with P21-mR-8R (20µg/ml) for a further 1 hour. This re-delivery was either immediate (0h) or with a 1-6 hour incubation between re-delivery before fluorescence analyses by flow cytometry. Immediate re-delivery is inhibited whereas >1 hour incubation between incubations allows the most efficient uptake of GET-protein. Error bars indicate s.d. n=6. * $p<0.05$.

Figure S28 GET of NEO promotes antibiotic-resistance in mouse embryonic fibroblasts. **(a)** Scheme of testing the antibiotic-resistance activity of transduced NEO (Neomycin phosphotransferase) in mouse embryonic fibroblast (MEF) cells. MEF cells (300,000) were cultured in DMEM containing 10% (v/v) FCS and P21-mR-NEO-8R (0, 10 or 100µg/ml) for 3 days feeding with fresh media daily. G-418 was then added to media for a further 3 days with daily feeding of fresh media. **(b-e)** P21-mR-NEO-8R rescues MEF and NIH3t3 cells

from G-418 selection by conferring antibiotic-resistance. **(b-c)** P21-mR-NEO-8R maintains living cultures of MEFs under G-418 selection. **(b)** MEF cell numbers when supplemented with SIN NEO (to overexpress NEO) or transduced with P21-mR-NEO-8R and selected with G-418 (0, 75, 150 or 300µg/ml). **(c)** MEF cell numbers for the 150µg/ml dose of G-418. Error bars indicate s.d. **(d-e)** P21-mR-NEO-8R promotes viability in G-418 selected MEF and NIH3t3 cells. **(d)** Quantitation of the percentage of viable MEF cells using Trypan Blue staining. **(e)** Fluorescence microscopy of NIH3t3 cells selected with 150µg/ml G-418 assessed for viability using LIVE/DEAD staining. Scale bar, 100µm. Error bars indicate s.d. n=6.